

Norwegian University
of Life Sciences

Master's Thesis 2021 60 ECTS

Faculty of Chemistry, Biotechnology and Food Science

Distribution of perfluorooctanesulfonate (PFOS) isomers in a Norwegian arctic food web

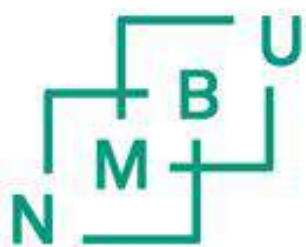
Fedor Lennikov

Chemistry

Preface

Distribution of perfluorooctanesulfonate (PFOS) isomers in a Norwegian arctic food web

This thesis was written at the Faculty of Chemistry, Biotechnology and Food Science (KBM) at the Norwegian University of Life Sciences (NMBU) in Ås, Norway with assistance from the Norwegian Institute of Marine Research (NIMR), Bergen. The laboratory work was carried out at the Faculty of Chemistry, Biotechnology and Food Science (KBM) and the Faculty of Veterinary Medicine (VET) at NMBU, Ås.



Norges miljø- og
biovitenskapelige
universitet



Fedor Lennikov

Ås, 31.10.2021

Acknowledgements

This thesis was written during the Covid-19 pandemic. It was completed under challenging circumstances, which would not have been possible without the assistance of the great people working here at NMBU. For this I am very grateful.

I would like to thank you all individually.

Supervisor Professor Roland Kallenborn, for giving me the opportunity to work with such an interesting subject and for all the help along the way.

Co-supervisor Adjunct associate Prof. Aasim Musa Ali, for constantly providing input and guiding me through the project.

Co-supervisor Postdoctoral researcher Ivo Havranek, for relentless assistance at the lab and in general.

Senior engineer Erik Magnus Ræder, for finding time to assist with transferring and setting up the analytical method on a new instrument, as well as for overseeing the analysis and transferring the analytical data.

I would like to thank everyone involved for their flexibility and willingness to help during times of lockdowns and social distancing.

This study was funded by the project PFOslo, NFR 268258 - Reducing the impact of fluorinated compounds on the environment and human health.

Abstract

Perfluorooctanesulfonate (PFOS) is a global synthetic fluoroorganic compound and one of the most abundant per- and polyfluorinated alkylated substances (PFAS) in the arctic environment. PFAS are ubiquitously dispersed throughout the planet's aquatic environments, soils and wildlife. Their environmental persistence, tendency to bioaccumulate and biomagnify in food webs coupled with negative health effects at elevated levels has resulted in them being commonly described as persistent organic pollutants. Although PFOS and other PFAS compounds have been subject to increasing scientific interest in the decades following their discovery, much remains unknown and uncertain in regards to their global and local transport mechanisms as well as their potential as environmental toxins.

The objective of this study was to develop and validate an analytical method for the separation and determination of the individual PFOS isomers commonly found in environmental and technical samples, and attempt to quantitate them in biota samples from Svalbard, Norway. Collected samples from neighbouring levels of the food web at two different locations in the vicinity of Longyearbyen were analysed for the purpose of gaining insight into the levels of the individual PFOS-isomers, and changes happening to the isomer profile from one trophic level to the next.

A new high performance liquid chromatography mass spectrometry (HPLC-MS/MS) analytical method was designed by combining elements from other published studies. The method was used to separate four groups of PFOS isomers from a mixture and was applied to quantitate PFOS isomers in the biota samples.

It was found that the total PFOS concentrations and the relative concentrations of L-PFOS in the biota samples increased with increasing trophic levels, in agreement with previous reports on the isomer's greater bioaccumulation tendency. Fish liver samples from a reference station without any known nearby local PFOS pollution sources were discovered to have higher total PFOS levels than fish liver samples from a station near a decommissioned fire-fighting station. However, a small sample size and uncertainty with regards to the quantitation made it hard to interpret the findings, as PFOS isomers at lower trophic levels were not detected due to insufficient sensitivity.

Sammendrag

Perfluoroktansulfonat (PFOS) er en syntetisk fluoroorganisk forbindelse og en av de mest utbredte per- og polyfluorinerte alkylerte stoffene (PFAS) i arktiske miljøer. PFAS er svært utbredt og er spredt over hele verdens akvatiske miljøer, jord og dyreliv. Deres persistente natur, tendens til å bioakkumulere og magnifisere i næringskjeder, samt deres negative helseeffekter ved forhøyede nivåer har gjort at de regnes som persistente organiske forurensningsstoffer. Selv om PFOS og andre PFAS forbindelser har vært gjenstand for økende vitenskapelig interesse in tiårene etter deres oppdagelse, er det fortsatt mye som ikke er kjent når det kommer til deres globale og lokale transportmekanismer og deres potensiale som miljøgifter.

Formålet med denne studien var å utvikle og validere en analytisk metode til separasjon og bestemmelse av de individuelle PFOS isomerene tilstede i miljøprøver og i teknisk produkt, og forsøke å kvantifisere disse i biota-prøver fra Svalbard, Norge. Sampleprøver fra nærliggende trofiske nivåer i næringskjeden fra to ulike lokasjoner i området rundt Longyearbyen ble analysert i et forsøk på å skaffe seg innsikt i mengdene av de individuelle PFOS-isomerene, og hvordan isomerprofilen forandrer seg fra ett trofisk nivå til det neste.

En ny analytisk HPLC-MS/MS metode ble utviklet ved å kombinere elementer fra andre publiserte studier. Metoden ble brukt til å separere fire grupper PFOS isomerer fra en blanding og ble brukt til å separere fire grupper PFOS-isomerer fra en blanding og ble så benyttet til å kvantifisere isomerer i biotaprøvene.

Det ble påvist at den totale PFOS konsentrasjonen og de relative L-PFOS konsentrasjonen i biotaprøvene økte høyere opp i næringskjeden, i samsvar med tidligere rapporten om isomerens større bioakkumuleringsegenskaper. Fiskeleverprøver fra en referansestasjon uten kjente nærliggende PFOS utslippskilder ble funnet å ha høyere total-PFOS konsentrasjoner enn fiskeleverprøver fra en stasjon nær en nedlagt brannøvelsesstasjon. Det lave prøveantallet og usikkerhet tilknyttet kvantifiseringen gjorde det vanskelig å tolke funnene, siden PFOS isomerer ikke ble kvantifisert ved lavere trofiske nivåer på grunn av utilstrekkelig sensitivitet.

Acronyms and abbreviations

Br-PFOS	Branched PFOS-isomers
ECF	Electrochemical fluorination
ESI	Electrospray ionisation
FFTS	Fire-fighting training station
GC	Gas chromatography
HPLC	High performance liquid chromatography
ISTD	Internal standard
LOD	Limit of detection
LOQ	Limit of quantification
L-PFOS	Linear PFOS-isomer
MRM	Multiple reaction monitoring
MS	Mass spectrometry
MS/MS	Tandem mass spectrometry
PCB	Polychlorinated biphenyls
PFAS	Poly- and perfluoroalkyl substances
PFOA	Perfluorooctanoic acid
PFOS	Perfluorooctanesulfonate
POP	Persistent organic pollutants
POSF	Perfluorooctanesulfonyl fluoride
PP	Polypropylene
QqQ	Triple quadrupole
SPE	Solid phase extraction
STD	Standard
WAX	Weak anion exchange

1. Introduction

1.1 Background and terminology

Per- and polyfluorinated substances (PFAS) are synthetic organofluorine compounds ubiquitously dispersed throughout the atmosphere, waters and soils in the world. It is a structurally diverse subsection of fluorine POP compounds with characteristics differentiating them from legacy perfluorinated compounds (PFC's), historically used as a broad term encompassing perfluorinated compounds (Chu & Letcher 2009). While the term PFC's has been used to refer to any perfluorinated organic compound regardless of chemical properties, structure and use, the term PFAS denotes a more specific class of compounds.

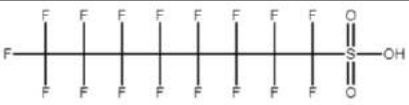
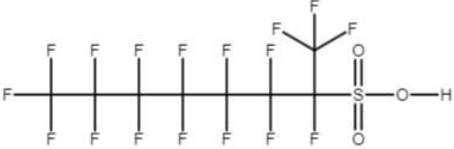
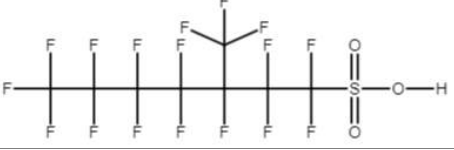
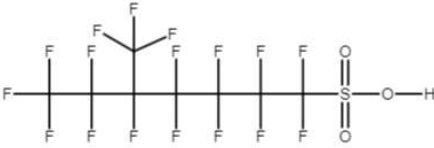
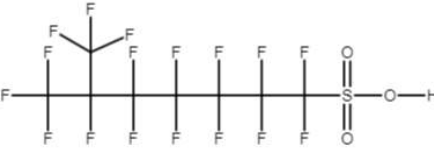
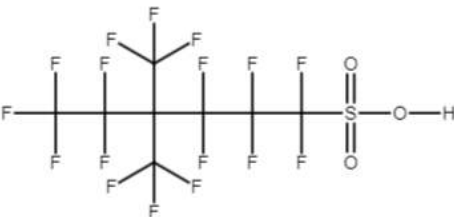
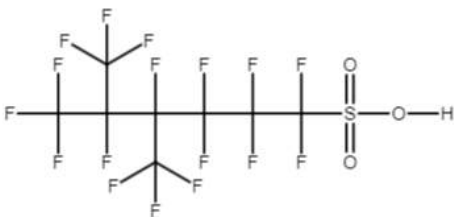
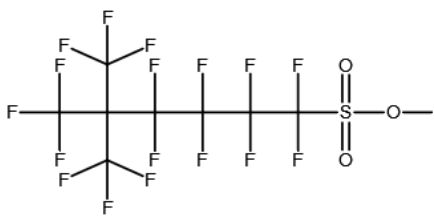
PFAS are compounds made up of a perfluorinated alkyl chain with the formula C_nF_{2n+1} and a functional group, typically a hydrophilic head (Buck et al. 2011). There is a great structural variety within PFAS, and the substances vary with regards to alkyl chain lengths, degree of branching and functional groups (Sturm & Ahrens 2010). The common characteristics for all PFAS is that they are aliphatic organic compounds with a saturated carbon chain with at least one, but often most all hydrogens have been replaced with fluorine atoms (Buck et al. 2011; Kissa 2001; Parsons et al. 2008).

PFAS compounds are synthetic and almost entirely anthropogenic in nature (Kissa 1994). Apart from a few short-chain exceptions they have been introduced to the environment either as direct industry pollutants or as their degradation products (Frank et al. 2002). This means that the vast majority of the PFAS in the environment is a result of anthropogenic pollution, and that the key to control the PFAS levels in the environment is by controlling the output, for instance through regulations.

Perfluorooctylsulfonic acid (PFOS) is a specific PFAS compound with the chemical formula $C_8HF_{17}O_3S$. It is made up of an 8-carbon perfluorinated alkyl chain and a sulfonate functional group (Chu & Letcher 2009). Perfluorooctylsulfonic acid can also exist as its deprotonated conjugated base, called perfluorooctylsulfonate. Throughout this thesis PFOS will mostly be used to refer to the compounds ionised form, since it is most common in the environment (Kissa 2001).

PFOS itself is structurally diverse, and although its linear isomer (L-PFOS) is most abundant in the environment, theoretically as many as 89 other geometric isomers are possible (Houde et al. 2008). Despite this large potential diversity only 11 isomers have been identified in technical PFOS products (T-PFOS), of which only 8 are currently commercially available as pure standards (Chu & Letcher 2009).

Table 1-1: Names, acronyms and chemical structures of the target isomers in the current study.

Target isomer	Acronym	Chemical structure
Perfluorooctanesulfonate	L-PFOS	
Perfluoro-1-methylheptane sulfonate	P1MHpS	
Perfluoro-3-methylheptane sulfonate	P3MHpS	
Perfluoro-5-methylheptane sulfonate	P5MHpS	
Perfluoro-6-methylheptane sulfonate	P6MHpS	
Perfluoro-4,4-dimethylhexane sulfonate	P44DMHxS	
Perfluoro-4,5-dimethylhexane sulfonate	P45DMHxS	
Perfluoro-5,5-dimethylhexane sulfonate	P55DMHxS	

The terminology of PFAS varies from source to source. The different PFOS isomers have also been referred to by different names and acronyms since the first studies on their levels in the environment were published in the latter half of the 2000s. To avoid ambiguity, a

prevailing terminology introduced by Chu & Letcher (2009) has been used throughout the current study with respect to the names and acronyms of the PFOS isomers. The 8 commercially available pure PFOS isomers will serve as the target analytes in the current study. Their names, structures and acronyms are presented in table 1-1.

PFOS compounds were initially industrially introduced in the 1950's by the 3M company (Prevedouros et al. 2006). PFOS was discovered to have unique amphiphobic properties and were therefore primarily used as fluorosurfactants (Kissa 2001). It was mainly used as an active ingredient in stain repellents, most notoriously a fabric protector called Scotchguard (Sanderson et al. 2009). Growing concerns over the compounds toxic and bioaccumulative properties, coupled with its environmental ubiquity and persistence at the end of the century forced the 3M company to phase them out of production from year 2001 (Place & Field, 2012).

In the decades following, PFOS have largely been replaced by new compounds in the Western world, such as shorter chain PFAS, whose environmental properties and toxicology are less known (Wang et al. 2013). However, PFOS continues to be produced in other parts of the world, such as China, and can be found in import products such as textiles and plastics. Additionally, the compound has been globally distributed through long-range transport mechanisms due to its chemical properties and environmental persistence, and is even known to exist in the environments of remote regions, such as the Arctic (Chu & Letcher 2009).

1.2 Physical and chemical characteristics

PFOS are characterised by their unique amphiphobic properties resulting from the combined effect of their lipophilic perfluorinated carbon chain and their hydrophilic sulfonate head (Moody & Field 2000). This characteristic enables them to effectively reduce the surface tension between liquids in direct contact and enable emulsification (Kissa 2001). The amphiphobic nature of PFOS has also been utilized for material surface protection in the form of coatings, to protect the material from degradation from exposure to water and lipids in the surroundings (Kissa 2001).

Although often referred to as acids, PFOS can be found both as anionic and protonated species at environmental pH values, significantly influencing their affinity for different environmental matrices, such as soils, waters and air (Kissa 2001; Conder et al. 2008). They have low vapour pressure, and are therefore generally little susceptible to vaporisation once dissolved in water or adsorbed in soils (Shoeib et al., 2006). As a result, they are less of an atmospheric pollutant than many other legacy PFC's, and are widely dispersed in soils and aquatic environments as well. Similarly, unlike legacy POPs, such as DDT, their bioaccumulation properties and persistence can't be easily predicted by partitioning coefficients such as the octanol-water coefficient (K_{ow}) (Chu & Letcher 2009). On the other hand, PFOS have greater affinity for protein-rich tissues than their lipophilic POP counterparts, especially the liver and blood (Dietz et al. 2008).

PFAS are highly persistent and stable in the environment, including in matrices such as waters, soils and wildlife (Kissa 2001). They are thermally and chemically stable due to the strong covalent bonding between the fluorine and carbon atoms in the alkyl chain, coupled with the strong electronegative shielding from the fluorine atoms surrounding the carbon skeleton structure (Smart 2001). These characteristics allow the compounds to persist and biomagnify in environmental food webs, increasing in concentrations at higher trophic levels (Chu & Letcher 2009).

The isomers of PFOS are very similar in terms of their physical and chemical properties. Since they only differ in the perfluoroalkyl chain structure, they have proven to be difficult to separate and determine individually by established analytical methods (Chu & Letcher 2009). Additionally, their trace levels in environmental matrices have made achieving an adequate sensitivity an additional challenge in developing a quantitative method (Chu & Letcher 2009). Their analytical signals are known to be influenced by matrix effects, and be subject to interferences due to the challenging separation. Although multiple isomer-specific determination attempts have been made in the past, it has been more common to crudely separate L-PFOS from the branched isomers (Br-PFOS), and report their relative contributions to total PFOS.

Although L-PFOS/Br-PFOS ratios can provide insights and can be used for elucidation of pollution sources, contributions from environmental precursors and transport mechanisms, multiple studies have shown that the different branched isomers have differing chemical and physical properties, and as a result of that different toxicology's, persistence and bioaccumulation potentials (Fang et al. 2016; Houde et al. 2008). Hence, although this simplified crude separation is useful and can be used to obtain insights into the PFOS isomer composition with it can also result in a lot of information on the specific isomers contribution to the isomer profile being lost.

1.3 Synthesis and uses

PFOS are like most PFAS compounds exclusively anthropogenic synthetic compounds (Kissa 2001). They have been historically used in coatings to protect and make materials such as textiles and paper more resistant against polar and organic compounds (Brooke 2004). PFOS compounds are still in use to this day and are present in some hydraulic fluids for aviation as well as fire-fighting foams (Seow 2014). Elevated levels of PFOS have been detected in numerous waste sites close to airports and fire-fighting stations.

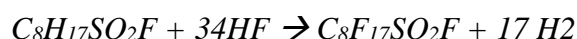
Historically two primary methods have been used for the industrial manufacturing of PFAS, such as PFOA – telomerization and electrochemical fluorination (ECF). The methods have different synthesis mechanisms and differ in the resulting isomer composition of the technical product (Prevedouros 2006). It should be noted that other methods for PFAS synthesis exist, but these are not known to have been used in large scale, and their contributions are therefore considered to be negligible. However, PFOS is different from PFOA and other PFAS compounds in that it has historically exclusively been synthesised by ECF (Kissa 2005).

PFOS industrially released into the environment from industry are therefore mainly ECF products.

ECF was a method first developed for large scale PFOS production by the Minnesota Mining and Manufacturing Company (now called the 3M company) in the late 1940's (Butt et al. 2010; Paul et. al 2009). ECF was the main method for PFOS synthesis throughout the 20. Century, and up until its phase-out from 2002. This method is based on free-radical reactions yielding a technical PFOS product with a $70 \pm 1.1\%$ L-PFOS isomer profile, while the remaining $30 \pm 0.8\%$ is made up of branched PFOS isomers (Vyas et al. 2007). It is an electrolysis method where a hydrocarbon precursor is immersed in anhydrous hydrofluoric acid and electrolysed, causing the replacement of the hydrogen atoms in the alkyl chain with fluorine (Kissa 2001). The process results in the creation of hydrogen gas as a by-product. Both organic carbon-hydrogen and carbon-carbon bonds are uncontrollably broken and replaced by carbon-fluorine bonds yielding a complex mixture of compounds, including branched PFOS isomers and shorter chained PFAS compounds (Prevedouros 2006). The number of shorter chained PFAS compounds has been shown to increase with time under voltage (Buck et al 2011).

A simplified reaction equation for 3M's synthesis of PFOS is presented in equation 1-1. 1-octanesulfonyl fluoride was historically used as the starting feedstock for the production of a mixture of perfluorooctanesulfonyl fluoride (POSF) isomers and homologues on reaction with the anhydrous hydrofluoric acid. POSF is then converted to PFOS through chemical hydrolysis as the terminal step in the process (3M Company 1999).

Equation 1-1: Equation showing the simplified sum reaction of the fluorination of 1-octanesulfonyl in HF, yielding perfluorooctanesulfonyl fluoride (POSF) and hydrogen gas as a by-product.



The use of ECF for the purpose of PFOS production has been largely phased out during the last two decades. In the years following, telomerisation became the primary method to synthesise PFAS compounds, including shorter-chained replacements for PFOS (De Silva & Mabury 2004).

Telomerisation is an alternative process of PFAS synthesis. This method was developed by the Dupont Company in the 1970's and is a more controlled and product-specific alternative. Telomerisation is a complicated multiple-step process where the alkyl chains are constructed from short carbon moieties (Kissa 2001). This allows for isomer-specific synthesis, resulting in pure products (De Silva & Mabury 2004). However, telomerisation is not suited for PFOS production, and thus PFAS synthesized by telomerisation do not influence the PFOS isomer profile in the environment (De Silva 2010).

1.4 Environmental relevance and risks of exposure

The toxicology and bioaccumulation properties of PFOS has attracted significant scientific interest in the past two decades. Due to the compounds wide-spread and persistent nature in different matrices such as soils, waters and biota it is considered a global pollutant (Ahrens 2011).

PFOS has been linked to negative health effects including disruption of immune and endocrine systems, liver and neonatal damage, and neurobehavioral changes (Post et al. 2012). Additionally, it has been shown to have carcinogenic properties in animal studies (USEPA 2014).

Giesy & Kannan (2001) published one of the first studies on the global distribution of PFOS, determining its presence and levels in wildlife tissues from a number of continents and documenting its global dispersion. The findings showed increasing levels of PFOS at higher trophic levels in food webs, indicating a tendency for bioaccumulation and biomagnification. The findings have been confirmed by a large number of studies since, providing additional insights into the compound's properties and behaviour in food webs, such as the ones in Arctic regions (Houde et al. 2008).

A study examining the extent of PFOS bioaccumulation in an eastern Arctic food web found a positive linear relationship between the PFOS levels and the trophic level, corresponding to a trophic magnification factor of 3,1, and suggesting that PFOS biomagnifies in the livers of marine mammals and seabirds (Tomy et al. 2004). In a later study, PFOS concentrations were found to be the highest in the livers of polar bears (*Ursus maritimus*), annually increasing in the sampling period of 1984-2006 (Dietz et al. 2008).

People in arctic regions with limited food sources are prone to dietary PFOS exposure. Eating from high trophic levels, where the PFOS concentrations are already built up can increase the risk of exposure and biomagnification, potentially leading to various adverse health effects. A study conducted by Hanssen et al. (2013) assessing delivering women's exposure to selected PFAS found the median PFOS plasma concentrations to be 11.0 ng/mL for women living in the Russian arctic, compared to 0.23 ng/mL for women from Uzbekistan. Elevated PFOS levels have been associated with chronic kidney disease, although this correlation has been disputed. Available research has not found a conclusively positive correlation between PFAS exposure and any clinically relevant birth outcomes. However, a lot remains unknown when it comes to PFOS and its effect on human health. Monitoring the levels and potential exposure is regarded as the most effective way of preventing negative health effects.

The impact of PFOS on people is further complicated by their differing isomeric compositions in the environment. The isomer profiles are in turn influenced by nearby sources, short-range and long-range transport and biological uptake and bioaccumulation properties. Zheng et al. (2019) recently examined the association between exposure to PFAS, and the exposure to L-PFOS and Br-PFOS specifically, and renal function in a population of adults residing in Shenyang, China. The study concluded that branched PFOS isomers were negatively associated with renal function, while L-PFOS was not. The effects of the individual branched isomers were not examined, but the research exemplifies that total PFOS

exposure is not always sufficient for accurate risk assessment, and that the health significance can be entirely decided by its isomeric make-up.

Similar isomer-related effects have been documented in arctic wildlife. The differences in branching results in different affinities to different tissues of arctic species. The relative concentrations of L-PFOS and select branched isomers among several tissues and blood of polar bears (*Ursus maritimus*) in Greenland were examined (Greaves et al. 2012). L-PFOS accounted for $93.0 \pm 0.5\%$ of total PFOS in the polar bear liver, compared to $85.4 \pm 0.5\%$ in the blood. Among the branched isomers, P6MHpS was the most dominant in the blood ($3.26 \pm 0.13\%$) and the liver ($2.61 \pm 0.10\%$), while no di-trifluoromethylated isomers were detected. The findings were assumed to be a result of differences in protein affinities, and hence rates of transport and absorption in the body. Similar isomer-patterns are unlikely to be exclusive to polar bears, further emphasising the need for adequate isomer-specific analytical methods.

Quantifying the isomers in different species in the same food web and different tissues within the same species could provide insights into both the species-specific pharmacokinetics, as well as the bioaccumulation propensity. Development of a fast, sensitive and isomer-specific method could potentially enable further research with regards to PFOS isomer-specific toxicity and accumulation. A complete isomer profile elucidation would then provide more accurate information on risk of environmental and health effects.

1.5 Sources and transport

The wide-spread distribution of PFOS throughout the world has been known for over two decades (Kissa 2001). However, a lot remains unknown with regards to the long-range transport mechanisms of this compound (Ahrens 2011). Despite the lack of local sources of PFOS in remote regions such as the arctic, it has been detected at alarming levels in water and biota samples (Chu & Letcher 2009). Insight into the sources and transport of the compound is essential to controlling the degree of harm brought by it to the environment. The PFOS isomer profile, relative levels of the different individual isomers and how its composition varies throughout the different local matrices can provide valuable information on the sources and transport of the compound.

Since PFOS are very resistant to chemical and physical degradation, their fate is typically deposition in environmental sinks. Adsorption to sediments and transport deep into the oceans are considered the largest sinks for PFOS in and around marine environments (Prevedouros et al. 2006). Since the production of PFOS has been significantly reduced in the last two decades, it is possible that if the rate of deposition in environmental sinks is higher than the rate at which new PFOS compounds are introduced to the environment, the total levels of PFOS in the environment will decrease (Paul et al. 2009). However, these transport mechanisms happen at such large scale that this is difficult to estimate precisely. The amounts of PFOS currently being produced are unknown, and it is presumed that most production is taking place without regulations or tracking. Additionally, determining the rates

of PFOS deposition requires great insight into the current concentrations throughout the different matrices and different regions. As a result of that, realistically only local changes to the isomer levels in different matrices can be determined and monitored, while the total global PFOS levels and the changes to it in the environment remain a dark figure.

The abundances of the different PFOS isomers is also subject to geographical variations. Due to differences in physical and chemical properties such as hydrophobicity, acidity and affinity for different matrices, different isomers have different rates of transport through the environment (Young et al. 2007). An example of this is their aforementioned reported differences in bioaccumulation properties.

The topic of the mechanisms of long-range transport of PFOS and PFOS precursors to arctic regions has been disputed in the two decades since the beginning of PFOS analysis in environmental samples. Due to their detection in matrices like water, wildlife and snow at levels beyond what local sources can account for, long-range transport was early proposed as an explanation for the findings. Two main PFOS transport mechanisms have been proposed – the slow and direct ocean transport (Armitage et al. 2006; Wania 2007) or the indirect atmospheric transport through volatile decomposing precursors and their subsequent deposition (Ellis et al. 2003; Shoeib et al. 2006).

Direct PFOS transport to the arctic is known to happen either by oceanic currents or by sea-spray aerosols. In a 2006 study Armitage et al. concluded that ocean water transport of PFO to the Arctic is an important pathway, contributing a yearly net influx of 8-23 ton – a contribution approximately one order of magnitude greater than the estimated PFOA transport through indirect sources, such as degradation of precursors and atmospheric transport. A similar study conducted by Buck et al. (2006) estimated an annual PFOA influx of 2-12 tons, which is significantly less than the former study, yet still more than the amount estimated to result from atmospheric transport. Later studies have since reported similar findings with regards to PFOS.

Atmospheric transport is another pathway of PFOS transport to the Arctic. Volatile fluorosulfamido alcohols can be atmospherically transported over great distances prior to oxidation, whereupon they are transformed into PFOS and deposited due to decreased volatility (Young et al. 2007). Several attempts at estimating the PFOS influx to the Arctic through atmospheric transport have been made. Young et al. (2007) estimated the magnitude of the atmospheric transport by studying PFOS concentrations in ice cap samples, and reported an influx of 18-48 kg annually. Although these numbers are smaller than those estimated for the oceanic transport, atmospheric transport is still considered an important primary pathway for PFOS to the Arctic. Another estimation of the PFOS contributions from local sources and long-range transport was made in 2013 in a study that found that long-range atmospheric transport was the major source of PFAS deposition on glaciers (Kwok et al. 2013). The findings are illustrated in figure 1-1.

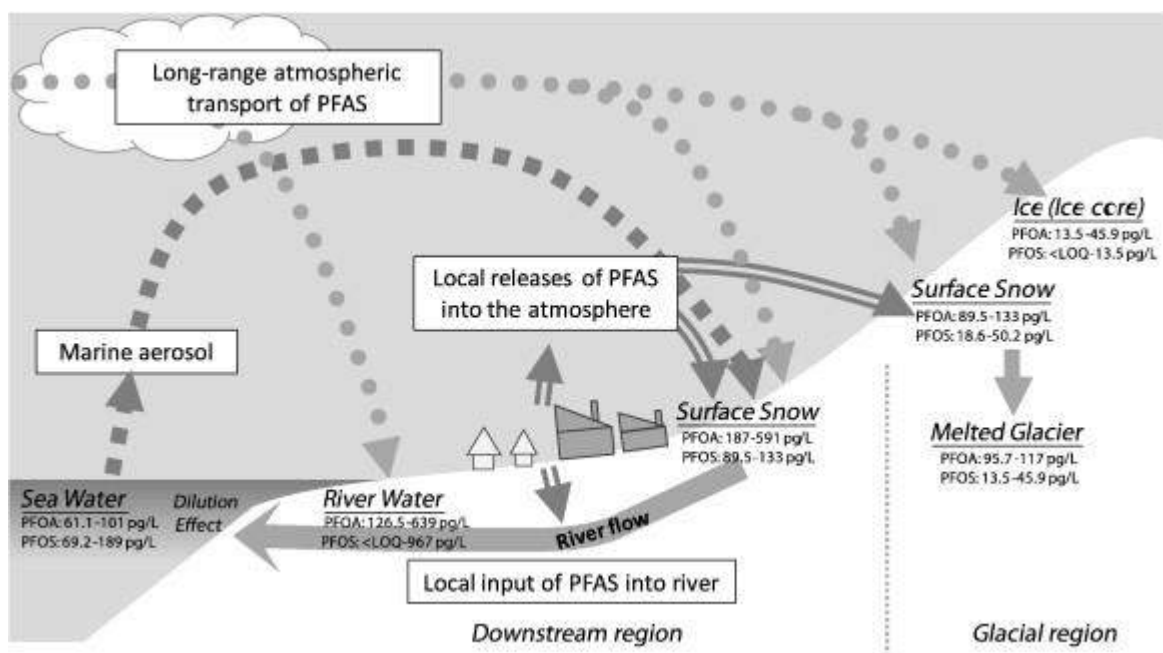


Figure 1-1: Illustration of the PFAS transport cycle in Svalbard, with estimated PFOS and PFOA contributions from atmospheric transport, reprinted with permission from Elsevier (Kwok et al. 2013).

The isomer profiles of PFOS in snow and lake water samples can be used to elucidate the contribution of different isomers from atmospheric transport. Branched PFOS isomer precursors have been found to degrade at a faster rate than L-PFOS precursors (Benskin et al. 2010). A number of studies have reported enrichment of br-PFOS in natural waters as compared to technical products (Benskin et al., 2010; Chen et al., 2015). Comparisons of the relative amounts of Br-PFOS in samples can therefore be used to infer the relative contributions from direct PFOS transport and indirect degradation of precursors.

The isomer profiles in biota samples are generally considered to be more indicative of the biological mechanisms and preferences for uptake, accumulation and degradation of the isomers. The current study will only examine PFOS in biota samples, making it difficult to comment on their mechanisms of transport.

1.6 Regulations

PFOS production has been in steady decline since the start of the century. The primary US manufacturer 3M voluntarily initiated their phase out of PFOS production following reports on its adverse environmental effects. In 2006, eight additional major PFAS manufacturing companies pledged to phase out the production of PFOS and PFOA and related chemicals by 2015. In 2017 the United States Environmental Protection Agency (USEPA) expressed concern of use of PFOA derivatives from other companies not participants of the PFOA stewardship program, and thus did not report baseline data on emissions and product content.

Additionally, imported goods from countries not subjected to PFOS and PFOA restrictions was noted as a potential risk of exposure.

PFOS is only one of the many PFAS compound being subject to strict global regulations. PFOS and its derivatives are currently globally regulated through the Stockholm Convention on Persistent Organic Pollutants. This is an international environmental agreement effective since May 2004 seeking to restrict, phase out and eliminate select global POPs. Although originally signed in May 2001, at a time when the persistence, ubiquity and toxicity of PFOS had largely become public knowledge, the compound wasn't included on the list of priority POPs before 2009, when it was listed under annex. B (UNEP 2009). This category consists of POPs that the different parties pledge to restrict. The official reported reasons for its addition in 2009 was increasing evidence of its persistence and bioaccumulation properties and adverse health effects, as well as the possibilities of long-range transport.

Since the addition to the Stockholm Convention in 2009 the use and production of PFOS, some of its derivatives and PFOSF have been globally restricted, apart from a few specific exceptions (UNEP 2009). Some of the exceptions are use in photo-imaging, aviation hydraulic fluids, metal plating's and certain medical devices. The treaty does not differentiate between the different PFOS isomers, and restricts the compound in general.

In Europe the use of PFOS has been restricted since 2007. The decision was made on the basis of information available by July 2002, indicating that the substance is persistent, bioaccumulative and toxic to mammalian species. The Scientific Committee on Health and Environmental Risks (SCHER) was consulted, supplying that the compound fulfilled the criteria for being considered as persistent organic pollutants (POPs). The directive expressed a need for further research, but a need for risk reduction measures was stressed. The member states pledged to apply the agreed upon measures by June 2008 restricting use of PFOS, with the notable exceptions in critical uses in the aviation industry, semiconductor industry and the photographic industry.

Despite evidence of isomer-specific toxicity and bioaccumulation potential, no international restrictions differentiate between the types of isomers in question. Instead, the restrictions encompass all PFOS isomers, as well as some of its salts and derivatives.

1.7 Isomer-specific analysis methods

Isomer-specific quantitation of the isomers in PFOS technical product was first attempted using ^{19}F NMR spectroscopy, but this technique was abandoned due to issues with sensitivity and interference from other fluorine-containing compounds in environmental matrices. Later attempts were exclusively based on chromatographic separations.

Gas chromatography (GC) showed promise as it was generally efficient at separating the PFOS isomers. However, PFOS are not volatile compounds, and must be derivatised into more volatile derivatives prior to GC-separation. Langois et al. (2007) made one of the first

attempts to derivatise PFOS isomers by catalysed esterification for GC, but achieved poor quantitative derivatisation. Chu & Letcher (2009) developed the first successful quantitative determination method for all 11 isomers in environmental samples using GC-MS. The process involved in-port derivatisation with tetrabutylammonium hydroxide (TBAH) in diethyl ether. The method was successfully applied for quantifying all target PFOS isomers in technical product, as well as some in arctic biota samples.

Liquid chromatography electrospray tandem mass spectrometry has historically resulted in better sensitivity than GC, but achieving an adequate isomer-specific chromatographic separation has been challenging. In 2017 Zhang et al. developed a new UHPLC-MS/MS and successfully used it to separate and detect 8 PFOS isomers in biosolids, biosolid-amended soils and plants (Zhang et al. 2017). This demonstrated that HPLC was a viable alternative for isomer-specific separation in environmental samples. The method has not been attempted on other environmental matrices.

1.8 Aim of the study

The aim of the current study was to attempt to develop and validate an analytical ESI-HPLC-MS/MS for the isomer-specific determination of PFOS. This was attempted through the combination, modification and improvement of existing published methods, to make it more suited for this objective, as well as the available instruments.

Additionally, the goal was to utilize this new method for the isomer-specific PFOS determination in Arctic biota samples from Svalbard, Norway. The selected biota samples were from different trophic levels, so that the analysis could provide some insight into the changes to the isomer profile throughout the local arctic food web.

Due to the PFOS isomers often yielding identical product ions following MS/MS fragmentation, an adequate chromatographic separation is integral for their isomer-specific quantitation. In 2017 Hu et al. achieved a complete isomer-specific HPLC separation of 10 target PFOS isomers with a perfluorinated C8 Epic FO LB column. With the goal of recreating this separation, the same column and gradient was adopted for use in the current study, as well as some other chromatographical parameters.

Mass spectrometry parameters are often specific to the instrument model, and similar settings on different instruments could yield different results. This makes adaptation difficult, and the parameters should ideally be optimised on the instrument in question with the target compounds in mind. However, due to time and access limitations the MS parameters were largely adopted from a separate quantitative PFAS method developed and optimised for the Agilent 6460 triple quadrupole HPLC-MS/MS system, similar to the system used in the current study. This reference method was not isomer-specific, and parameters related to the isomers, such as retention times and MS-settings were added.

Recently Ali et al. (2021) studied the fate of PFAS-compounds in a marine food web in Svalbard. The background PFAS levels, as well as the impact of local PFAS pollution

sources were explored. The current study attempted to quantitate the different target PFOS isomers in selected samples from this reference study. An exploration of the isomeric composition changes in the food web not influenced by nearby pollution sources would allow for better assessment of the different isomer's bioaccumulation and magnification properties.

2. Materials and methods

2.1 Chemicals and materials

A complete overview of all standards, reagents and materials used is presented in appendix B. The reagent solutions used in the sample preparation were prepared as follows.

0.1% ammonium hydroxide solution was prepared by diluting 2 mL of 25% ammonium hydroxide in 498 mL of methanol in a 500 mL volumetric flask.

25 mM ammonium acetate buffer was prepared by weighing 1.93 g of ammonium acetate and dissolving it in a 1 L volumetric flask filled with Milli Q water.

50/50 (v/v) solution of methanol/10 mM ammonium acetate in Milli Q water was prepared by weighing 0.193 g of ammonium acetate and dissolving it with Milli Q water in a 250 mL volumetric flask. The solution was then transferred to a 1.0 L glass beaker, and mixed with 250 mL of methanol.

10 mM ammonium formate buffer was prepared by weighing 0.631 g of ammonium formate and dissolving it in Milli Q water to a final volume of 1000 mL using a volumetric flask, prior to transfer to a glass beaker.

2.2 Study site

Svalbard is an archipelago in the Norwegian Arctic, approximately 2000 kilometres north of mainland Norway. Figure 2-1 shows a map of the entire archipelago. The mean temperature in Longyearbyen in the period 1971-2000 was -5.9 °C, ranging from an average of -14.0 °C in the winter to +4.5 °C in the summer. The temperature has been reported to increase since 1970, expected to increase between 4.0 °C and 5.3 °C by the middle of this century. These changes are predicted to have dramatic consequences for the Arctic wildlife inhabiting the area.

The area of interest in the current study is the fjords surrounding Longyearbyen in Svalbard Norway. Longyearbyen is Svalbard’s largest settlement and home to an approximate 2400 permanent inhabitants, in addition to hosting up to 100 000 tourists on a yearly basis in the years leading up to 2018. The primary means of long-range transport to and from the settlement are by cruise ship or by airplane. Automobiles and snowmobiles are popular as local means of transportation.



Figure 2-1: Map of the Svalbard archipelago, from Tematisk Svalbard (NPI 2021).

A number of studies on PFAS, including PFOS, has been conducted in Svalbard since the discovery of their ubiquitous dispersion. Being a remote archipelago, the PFAS levels in Svalbard are sums contribution from long-range transport and local output. In 2005 studies on the levels of perfluoroalkyl contaminants in polar bears (*Ursus maritimus*) (Smithwick et al. 2005) and in glaucous gulls (*Larus hyperboreus*) (Verreault et al. 2005) were conducted, finding PFOS concentrations of 756-1290 ng/g (ww) in polar bear livers and 48.1-349 ng/g (ww) in the plasma of gulls, PFOS being the predominant PFAS contaminant. The PFOS levels in the arctic food web at Svalbard have been monitored since.



Figure 2-2: Photograph of Longyearbyen and Adventfjorden, where some of the samples were collected (npolar.no).

A number of local PFOS sources were previously identified in the Longyearbyen area. These include two point sources in Svalbard Airport (N 78°14', E 15°30') northwest of the settlement, and a decommissioned landfill in Adventdalen (N 78°10', E 15°56'), at the opposite side of the settlement. The airport has two fire-fighting training stations (FFTS) on either side. The FFTS located southeast of the airport is new and still in use, while the other one located north-east of the airport is decommissioned. Wastewater from the airport and the settlement is discharged into the Adventfjorden without treatment, contributing to the PFOS levels in the marine environment as a diffuse source.

The samples forming the basis of the current study were originally collected for the purpose of studying the fate of poly- and perfluoroalkyl substances in a marine food web influenced by land-based sources in the Norwegian Arctic (Ali et al. 2021). Information on the samples, sampling locations and methodology are therefore for the most part recited from this reference study.

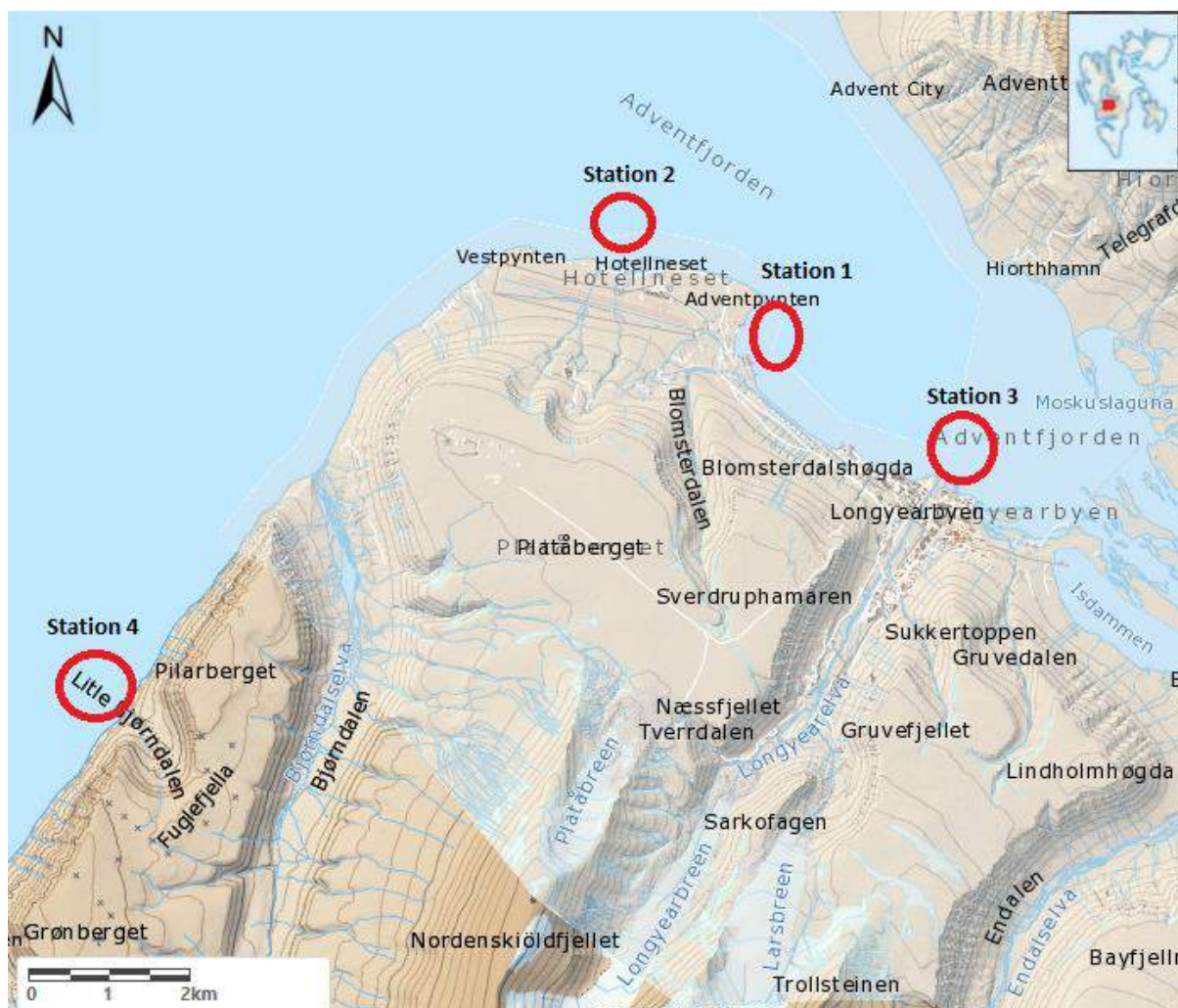


Figure 2-3: Geographical overview of the different sampling stations in the Longyearbyen area (Ali et al. 2021), from *Tematisk Svalbard* (NPI 2021).

Ali et al. (2021) attempted to examine the sources, levels and fate of select PFAS compounds in water, sediment and biota in the vicinity of Longyearbyen. The samples were collected at defined sampling stations, shown in figure 2-3. Stations 1-3 were used to measure the contribution of local pollution sources to the PFAS profile in Adventfjorden, while station 4, located in Isfjorden, was used as a reference station. The local sources were an active FFTS impacting station 1, an old and decommissioned FFTS impacting station 2, while station 3 was located next to Longyearbyen, and affected by the decommissioned landfill as well as the settlement in general. Station 4, located in Isfjorden, was approximately 10 km from any known PFAS source and was assumed to not be impacted by these local pollution source, and was therefore treated as a reference for background PFAS concentrations (Ali et al. 2021).

2.3 Sampling locations and sample selection

The marine biota samples used in the current study were collected in April 2018 (Ali et al. 2021). Samples were collected at all four sampling stations. The current study is primarily centred around the PFOS isomer profiles in a food web undisturbed by local sources. For this reason mainly samples from reference station 4 in figure 2 were analysed. Fish liver samples from station 2 were also selected for this study for isomer profile comparison.

3 replicates of a pelagic zooplankton (copepods, such as *Calanus* spp.) sample collected from station 4 was selected, and represents the lowest trophic level examined in this study. In addition, 4 individual crab samples (*Hyas araneus*) and 3 fish liver samples (sculpin - *Myoxocephalus scorpius*) from station 4 were selected.

Glaucous gulls (*Larus hyperboreus*) were sampled from the area around Svalbard airport – in between stations 1 and 2 on land. 4 gull liver samples obtained from these were selected and used in the current study. Gulls represent the highest trophic level in this study. Although no gull samples from the area around station 4 were available, it was still expected that the isomer profile in gull livers would provide information on the bioaccumulation potentials of the different individual PFOS isomers.

At last, 3 fish liver samples from station 2 were selected to allow for the comparison of the isomer levels at different locations from the same trophic level. The aim was to obtain some insight into how the local pollution source (the decommissioned FFTS) would impact and change the isomer profile in fish livers.

2.4 Transport and storage

After sampling each fish and gull liver sample was wrapped in two layers of aluminium foil to prevent contamination from the surroundings, as well as from cross-contamination from other samples. Zooplankton and crab samples were stored in 15 mL PFAS polypropylene tubes free of PFAS. The sample contents, locations and dates were written on the foil for documentation purposes.

The samples were transported to KBM at NMBU in Ås and stored in a freezer at temperatures below -18°C. They were stored there the entire period up until sample preparation in the months of May and June 2021.

2.5 Sample preparation

The entire sample preparation procedure was carried out at KBM at NMBU, Ås. The preparation method was a modified SPE WAX extraction followed by ENVI-carb clean-up and spin-x filtering prior to analysis. This was based on established guidelines for PFAS

sample preparation, with some modifications (Ahrens et al. 2010). ENVI-carb clean-up was included to remove lipids from the samples, while spin-x filtering was included to remove the remaining ENVI-carb particles, as well as other particulate matter in order not to damage the HPLC-MS/MS system.

The samples were prepared in batches of 10-20 at a time, batch size limited by the vacuum manifold capacity. A minimum of two blank samples spiked with ISTD were prepared alongside the samples in each batch as procedural blanks.

2.6 Pre-treatment

The frozen samples were thawed at room temperature overnight in preparation for extraction. Samples stored in polypropylene falcons (zooplankton and crabs) were homogenised by extensive stirring using a laboratory spatula, until a uniform consistency was achieved. Solid samples stored in aluminium foil (fish and gull liver) were first transferred to a porcelain bowl, which had been cleaned with 70% ethanol. They were ripped into smaller pieces using two spatulas and stirred until homogenised prior to weighing. The porcelain bowl was rinsed with water and wiped clean with 70% ethanol using a paper towel between after each individual sample was homogenised.

The samples were weighed prior to extraction. An empty 15 mL polypropylene falcon tube was placed on the weight and tared. Then the contents of each individual sample were transferred to the empty falcon tube until the weight read 0.9-1.3 g. The exact weight for each individual sample was documented in the sample protocol.

Each weighed sample was added 50 ng isotopically labelled internal standard (50 µL from a 500 ng/mL ISTD solution). The samples were then extracted.

2.7 Extraction

Each sample was added 10 mL of acetonitrile and mixed using a vortex mixer for 60 seconds. The falcon tubes were then transferred to an ultrasonic bath and sonicated for 30 minutes at room temperature to extract the PFOS compounds from the sample material.

Following sonication, the samples were centrifuged at 2500 rpm for 5 min. The supernatant was decanted into new empty 15 mL polypropylene tubes, dried by nitrogen evaporation and then redissolved in 5 mL of Milli Q water by 60 seconds of vortex mixing.

2.8 SPE WAX extraction

The samples were extracted by means of weak anion exchange extraction (WAX), a type of solid phase extraction (SPE) technique traditionally used for the extraction of PFAS compounds. The WAX cartridges were positioned on a vacuum manifold and the following standardised three-step procedure was carried out.

The WAX SPE cartridges were conditioned by 4 mL of 0.1% ammonium hydroxide in methanol, followed by 4 mL of pure methanol and 4 mL of Milli Q water. The samples dissolved in 5 mL of Milli Q water were then loaded onto the WAX cartridges, and the valves were adjusted to a flow of approximately one drop per second to ensure the analytes had sufficient time to absorb to the resin. After that the cartridges were washed with 4 mL of 25 mM ammonium acetate in Milli Q water, and eluted with 6 mL of methanol followed by 0.1% ammonium hydroxide in methanol and collected in test tubes. They were transferred to 15 mL polypropylene falcon tubes immediately following the collection prior in preparation of the next step in the procedure.

2.9 Clean-up (ENVI-Carb)

After extraction, the samples were dried by nitrogen evaporation, dissolved in 1.5 mL of acetonitrile by vortex-mixing for 60 seconds and incubated in an ultrasonic bath at room temperature for 5 minutes. For clean-up, each sample was added approximately 50 mg of activated carbon (ENVI-carb) and vortex-mixed for 60 seconds again.

The samples were then centrifuged at 10 000 rpm for 10 minutes and the acetonitrile with the extracted PFOS analytes was decanted into new 15 mL polypropylene tubes, before being nitrogen evaporated to dryness again. The dried extracts were added 500 μ L of 50/50 (v/v) methanol/10 mM ammonium acetate, vortex-mixed for 60 seconds and sonicated in an ultrasonic bath at room temperature for 5 minutes to dissolve the compounds prior to filtering.

2.10 Filtering

Each sample was transferred to a separate spin-x vial and centrifuged at 12 500 rpm for 3 min. The filters were removed and the samples were transferred to new vials for HPLC analysis.

2.11 Instrumental analysis

The instrumental method development, validation and analysis was carried out at the Faculty of Veterinary Medicine (VET) at NMBU in Ås, Norway.

The method was developed by adopting parts of published HPLC-MS/MS methods and altering the method to better suit the available instruments. The chromatographic parameters and gradient were adapted from an isomer-specific PFOS study (biosolids). The MS-parameters were largely adapted from a study on elucidation of contamination sources for PFAS on Svalbard using the same instrument setup as the current study (apart from the chromatographic column) (Skaar et al. 2019). Adjustments were made to modify the method into an isomer-specific MRM method. A complete list of the method parameters is supplied in appendix C.

The setup used for analysis was an Agilent 1200 HPLC system coupled with an Agilent 6460 triple quadrupole (QqQ) mass analyser (MS/MS). An Epic FO LB column (1.8 μm , 120 Å, 2.1 mm \times 150 mm, ES Industries) was used for the isomer-specific chromatographic separation.

2.12 HPLC separation and identification of analyte isomers

The HPLC-MS/MS analysis was carried out at the Faculty of Veterinary Medicine (VET) at NMBU in Ås. Since the goal of the study was to develop an isomer-specific method for HPLC-MS/MS PFOS isomer determination, the main requirement of the chromatographic separation was a resolution sufficient for the quantitative analysis of samples consisting of all of the analyte isomers. The fact that the different PFOS isomers tend to have similar, overlapping mass transitions, effectively meant that a complete separation of the individual isomers was necessary for quantitative determination of all analytes.

The analyte isomers were identified based on their retention times following individual injection. Once their different retention times were known, their peaks could be identified in a PFOS mixture, and in the subsequently analysed biota samples.

Zhang et al. (2007) were successful in achieving a complete separation of the analyte isomers. In an attempt to reproduce the results, the already optimized HPLC separation parameters from the reference study were adapted and integrated into the current method. This included the use of the same perfluorinated Epic FO LB chromatographic column, with the column temperature set to 35 °C.

The standards and samples were injected in volumes of 10 μL at a constant flow rate of 150 $\mu\text{L}/\text{min}$, although the reference study used 5 μL injections. This was an adjustment resulting from low standard signals at concentrations below 5 ng/mL, sometimes indistinguishable from noise, during the individual standards testing.

The elution was performed with a binary gradient program consisting of mobile phase A (10 mM ammonium formate in Milli Q water) and B (methanol), shown in table 1. Individual runs had a duration of 45 minutes in total, the last 10 minutes being spent reconditioning the column at the initial mobile phase ratio. A complete list of the HPLC separation parameters is supplied in appendix C.

Table 2-1: The gradient elution program. Mobile phase A was 10 mM ammonium formate, while mobile phase B was pure methanol.

<i>Time (min)</i>	<i>A (%)</i>	<i>B (%)</i>
0	65	35
0.3	65	35
1.9	36	64
5.9	34	66
7.9	30	70
28	25	75
29	0	100
34	0	100
35	65	35
45	65	35

2.13 MS/MS detection and parameters

The PFOS target isomers were detected using an Agilent 6460 series triple quadrupole mass spectrometer. The MS-method was as mentioned largely adopted from a previous PFAS analysis study performed on the same instrument yielding adequate results (Skaar et al. 2019). However, since the method used in the reference study was not isomer specific, this part of the method had to be developed and integrated into the reference method. Individual isomer standards were injected and detected for mass transition screening using ESI Agilent jet stream mode, and some of the most abundant fragment ions for each isomer were selected for the MRM quantification method.

To assess the relative product ion abundances, an MRM method was used for screening using the same MS-parameters as the final MRM acquisition method used for quantification. 3-4 of the most abundant product ions for each target isomer were selected and adopted for the final MRM method. An additional requirement for product ion selection was that the selected ions had to differ from those of co-eluting isomers, meaning that if the signals of multiple isomers were not chromatographically resolved identical mass transitions could not be used for their individual quantification.

The 10 most common product ions were used for the MRM screening. The MS-parameters were not optimised for the target isomers, and the same parameters were used for each

transition. These included a dwell time of 30 ms, fragmentation energy of 200 V, collision energy of 61 V in negative polarity mode.

The general ion source parameters were also the same throughout the method development. These were adapted from the reference study (Skaar et. al 2019). The gas temperature was 300 °C and the gas flow was 5 L/min. The nebulizer operated with a pressure of 25 psi, and the capillary voltage was 2500 V. A complete list of the MS-parameters used is supplied in appendix C.

2.14 Contamination risk and control measures

Although the industrial production of PFOS has been largely phased out in the west in the past couple of decades, PFOS can be found in many imported commercial products, such as textiles, rubbers and plastic. PFAS compounds can also be found in the air and waters all over the planet at low concentrations. In addition to being a potential environmental and health concern, this poses a significant risk of contamination. Due to this concern, multiple anti-contamination measures were implemented throughout the duration of this analytical procedure.

All handling of samples and standards following storage has been done wearing nitrile gloves and a lab coat. All contact with plastics and other materials of unknown production origin was limited to the extent possible. Sample were at no point left uncovered while in PP tubes or test tubes throughout the sample preparation procedure. Procedural and instrument blanks were used to monitor potential contamination.

3. Quality assurance and method validation

3.1 Traceability

Prior to extraction all samples used in the current study were assigned a unique sample number and sample code, and tracked throughout the procedure. The sample code consisted of numbers and letters describing the type of biota sample it was, the sample number and what station it was sampled from, as well as if it was a replicate. The samples were also uniquely numbered based on the order in which they were weighed out for easier referencing throughout the procedure. In addition, the samples had unique sample run numbers, denoting the order in which they were injected and analysed by HPLC-MS/MS.

Both the sample number and the sample code were documented in the analytical protocol (appendix G) alongside information on the handling of each sample and additional comments regarding deviations from the described method. The exact weights of each sample were also documented there.

Instrument blanks, calibration standards and standard mixtures were not assigned sample preparation numbers or sample codes, as they didn't go through the same sample procedure as the rest of samples. Procedural blanks were treated as real samples and extracted next to them, and were therefore assigned sample preparation numbers, unlike instrument blanks.

3.2 Blank samples

Blank samples were used to track background levels of PFOS and their contribution to the levels of the target compounds in the method. In this method two types of blank samples were used – procedural blanks and instrument blanks.

Two procedural blanks were extracted in each batch alongside the biota samples. Empty polypropylene tubes were added ISTD and treated as regular samples throughout the procedure. Procedural blanks were used to track PFOS contamination throughout the sample preparation.

Instrument blanks were injected into the HPLC-MS/MS system to detect potential PFOS contamination and carry-over from samples earlier in the sample run. These were pure methanol blanks with no ISTD added, and were primarily used to monitor carry-over from samples earlier in the sample run.

3.3 Linearity and linear range

Calibration standards containing the target isomers at 6 individual concentrations of 0-20 ng/mL added 50 ng of ISTD were prepared. These were used to prepare calibration curves to assess the linearity of the response from the individual isomers. The linearity criteria were a regression curve R²-value of at least 0.99, and individual concentrations were excluded to satisfy this requirement, resulting in different linear ranges for the different analytes.

The concentration range of 0-20 ng/mL was selected based on the findings of total PFOS in different samples in the same area. Ali et al. (2021) found the PFOS concentrations to be approximately 0.10 µg/kg (w/w) in zooplankton, with levels at the different stations heavily influenced by local PFAS sources. These were expected to be the lowest concentration samples in the current study. Gulls are a high trophic level predator in the Arctic, and gull liver samples were therefore expected to contain much higher levels of PFOS. Ali et. al (2021) reported high individual variability in the distribution of PFAS, with an approximate median concentration of 30 µg/kg (w/w). Due to the current method being isomer-specific and due to limited amounts standards of individual isomer standards, the upper concentration limit was chosen to be 20 ng/mL.

3.4 Limits of detection and quantitation

Limits of detection (LODs) and limits of quantitation (LOQs) were calculated for each analyte. Co-eluting isomers that could not be distinguished based on retention times or MRM-transitions were treated as one target compound. Limit values were therefore calculated for these compounds as a group, rather than for each isomer individually.

The definitions and calculations of LOD and LOQ vary in the literature, and based on the definition there are multiple ways to calculate them. Herein, LOD was defined as the signal-to-noise ratio equal to 3, while LOQ was defined as the signal-to-noise ratio equal to 10, exemplified in equations 3-1 and 3-2.

Equation 3-1: The definition of LOD used in the current study.

$$LOD = \frac{3 \times \text{concentration}}{S/N}$$

Equation 3-2: *The definition of LOQ used in the current study.*

$$LOD = \frac{10 \times \text{concentration}}{S/N}$$

In practice, the limit values were calculated by plotting the (S/N) ratios the analyte in question produced for each calibration standard concentration, linearly regressing to get the slope and forcing it through the origin. The slope was then used to solve for the concentration, corresponding to the LOD or the LOQ value.

Equation 3-3: *LOD was calculated for each analyte by dividing 3 with the slope of the S/N ratios of their calibration standards plotted against concentration.*

$$LOD = \frac{3}{\text{slope}}$$

Equation 3-4: *LOQ was calculated for each analyte by dividing 10 with the slope of the S/N ratios of their calibration standards plotted against concentration.*

$$LOQ = \frac{10}{\text{slope}}$$

The limit values were used to determine whether the analytes in the current study were considered to be detectable and quantifiable based on the definitions used. Concentrations below LOD were treated as noise and determined to not be detected in the samples. Concentrations in-between the LOD and LOQ limits were determined to be detected, but not-quantifiable. If the sample concentrations were higher than LOQ, they were determined to be quantifiable as long as they were within the linear range, and thus could be calculated.

3.5 – Recovery

Recovery is an important metric in method validation providing a measure of the matrix effects on the analyte signals. The quantitation method used in the current study was an internal standard method. Only deuterated L-PFOS was commercially available, and thus only one internal standard was used for reference. The analyte PFOS were determined as ratios between the analyte signals and the L-PFOS ISTD. Since the different isomers have different chemical and physical properties, the extent to which the deuterated L-PFOS

internal standard is able to representatively correct for the matrix effects on their signals is unknown. This means that despite the isomeric nature of the target analytes in the current study, the matrix effects on the different analytes were treated as equal for all isomers. Recovery was calculated as a supplementary measure of the matrix effects influence on the individual target analytes, in an attempt to better assess the matrix effects on the individual analytes.

Recovery was calculated by preparing and determining the analyte concentrations in spiked recovery samples and with unspiked real samples. Three recovery replicates were prepared by spiking real samples with 1 ng of each target isomer standard after prior to weighing and the sample preparation procedure. They were then treated as real samples for the rest of the sample procedure, and used to calculate the recovery. Replicate spiked recovery samples were prepared from the following samples: zooplankton from station 4, crabs from station 4, and fish liver from station 2.

Recoveries were calculated with equation 2 using the calculated concentrations of the different target PFOS analytes in the samples. Average concentrations in the spiked replicates and average concentrations in the unspiked reference samples were quantified using the internal standard method, while the added concentration was known (2 ng/mL).

Equation 3-5: The equation used to calculate the recovery for each of the analytes.

$$\text{Recovery \%} = \frac{c(\text{spiked}) - c(\text{unspiked})}{c(\text{added})} \times 100\%$$

Acceptable recovery range for this method was set to be 40-120%, as one of the validation criteria in this method. Percentage values outside this range were considered unacceptable with regards to recovery for the target analyte in question.

3.6 Quantitation and data handling

The target isomer concentrations in the samples were calculated by the internal standard method. Calibration curves were created by plotting the ratios of analyte signal to internal standard signal on the y-axis against the concentration in the calibration standards, and then using linear regression to get calibration curve equation. The calculations were done automatically through Masshunter software version 10.1, and the data was then exported.

The isomer profiles in the different types of biota samples were calculated by using the median concentrations of the target analytes in the samples. These profiles could then be compared and changes to the isomeric make-up could be observed. Concentrations below

LOD were treated as zero, while concentrations higher than LOD, but lower than LOQ were treated as 0.5xLOQ.

If multiple isomers weren't completely chromatographically resolved, they were quantified together in groups with the coeluting analytes.

4. Results

4.1 Chromatographic separation and analyte selection

The chromatographic separation of the target PFOS isomers was only partial, and several isomers coeluted. The coeluting isomers shared physical and chemical characteristics due to similar alkyl chain structure. L-PFOS and P6MHpS were individually separated. The remaining monomethylated isomers coeluted in one peak, and the dimethylated isomers coeluted in another. The separation is shown in figure 4-1.

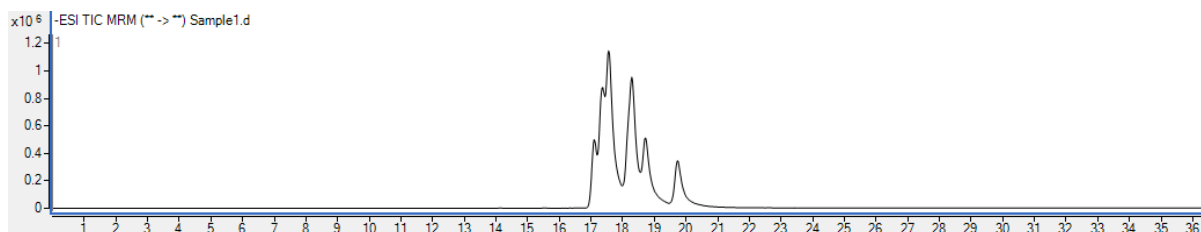


Figure 4-1: The separation achieved of the 8 target analyte isomers, here injected at 20 ng/mL.

Similar product ions means that isomer-specific determination was not possible with the described method. Hence the four separate chromatographical peaks were treated as 4 target analytes in the calculations. New analytes were defined by this separation – L-PFOS, P6MHpS, the monomethylated coeluting isomers P-1/3/5-HpS and the dimethylated coeluting isomers P-44/45/55-DMHxS. The latter two were groups of isomers validated and quantified as analyte groups, and were treated as individual analytes in the study.

4.2 Findings

Table 4-1 shows an overview of the findings. No PFOS isomers were detected in the zooplankton samples, only L-PFOS was detected in one of the crab samples. In fish livers all analytes were consistently detected, except from the branched analytes P-44/45/55-DMHxS.

The median quantified analyte concentrations in fish liver samples from station 2 were in the range 0.24-0.96 µg/kg. Fish liver samples from station 4 had somewhat higher levels in the range of 0.40-2.5 µg/kg. Gull liver samples, representing the highest trophic level, had the highest median concentrations at 0.16-66 µg/kg. Gull liver is the only sample type where the dimethylated isomers were detected and quantified in all samples.

Figure 4-2 shows a chart over the findings. It illustrates that the PFOS concentrations were significantly higher in gull liver than in the other sample types. L-PFOS dominates the isomer compositions in fish liver and gull liver samples, and is detected at increasingly higher concentrations at higher trophic levels.

Figure 4-3 shows the percentage contribution of the analytes to the PFOS isomer profiles in each sample type from the specific stations. The chart shows how L-PFOS increases percentage-wise at the higher trophic levels. The opposite trend is observed with the other monomethylated analytes, decreasing in terms of percentage contribution at higher trophic levels. Dimethylated isomers are barely detected at all, and only barely visible in the gull sample chart.

Table 4-1: Overview over the median concentrations and ranges of the different analytes in µg/kg.

Analyte	Zooplankton St4		Crab St4		Fish liver St 2		Fish liver St 4		Gull liver	
	n = 3		n = 4		n = 3		n = 3		n = 4	
	Median	Range	Median	Range	Median	Range	Median	Range	Median	Range
L-PFOS	nd.	nd.	nd.	nd - 0.15	0.96	0.78–1.6	2.5	2.2 – 2.7	66	28 – 183
P6MHpS	nd.	nd.	nd.	nd.	0.029	nd. – 0.044	0.088	0.069 – 0.14	2.4	0.69 – 9.8
P-1/3/5-MHpS	nd.	nd.	nd.	nd.	0.24	0.21 – 0.27	0.40	0.26 – 0.44	4.5	2.0 – 27
P-44/45/55-DMHxS	nd.	nd.	nd.	nd.	nd.	nd.	nd.	nd. – 0.24	0.16	0.13 – 0.59

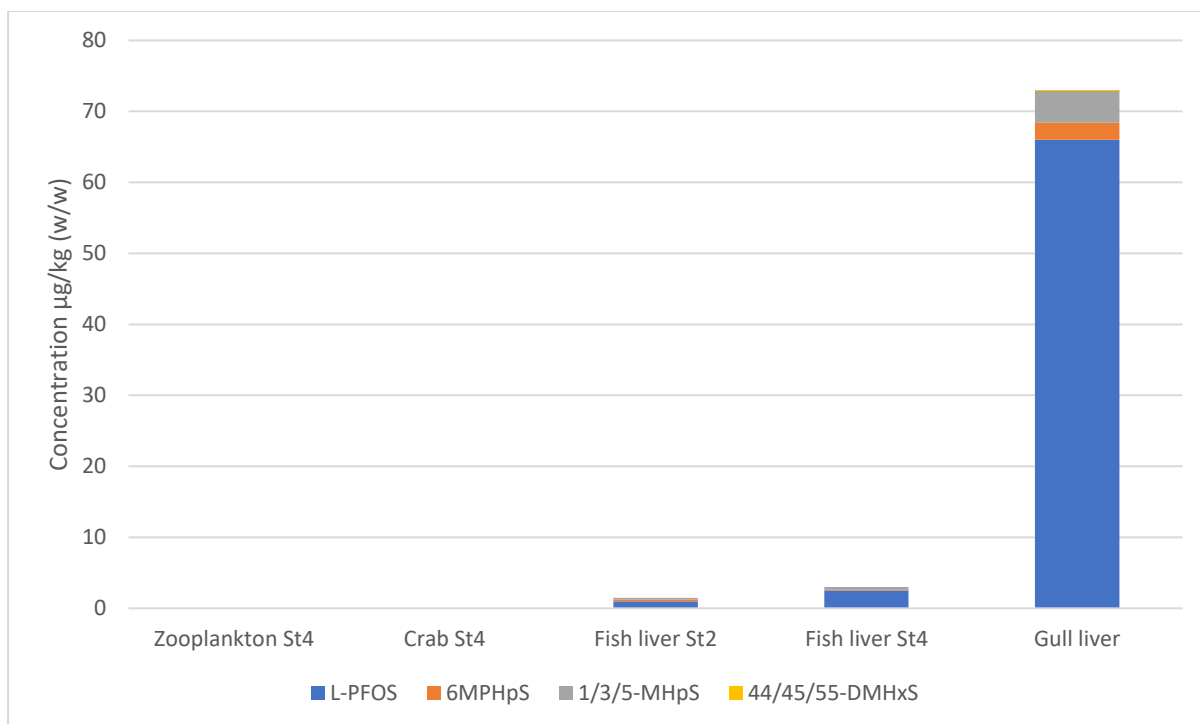


Figure 4-2: Chart overview of the median concentrations from each sample type and station.

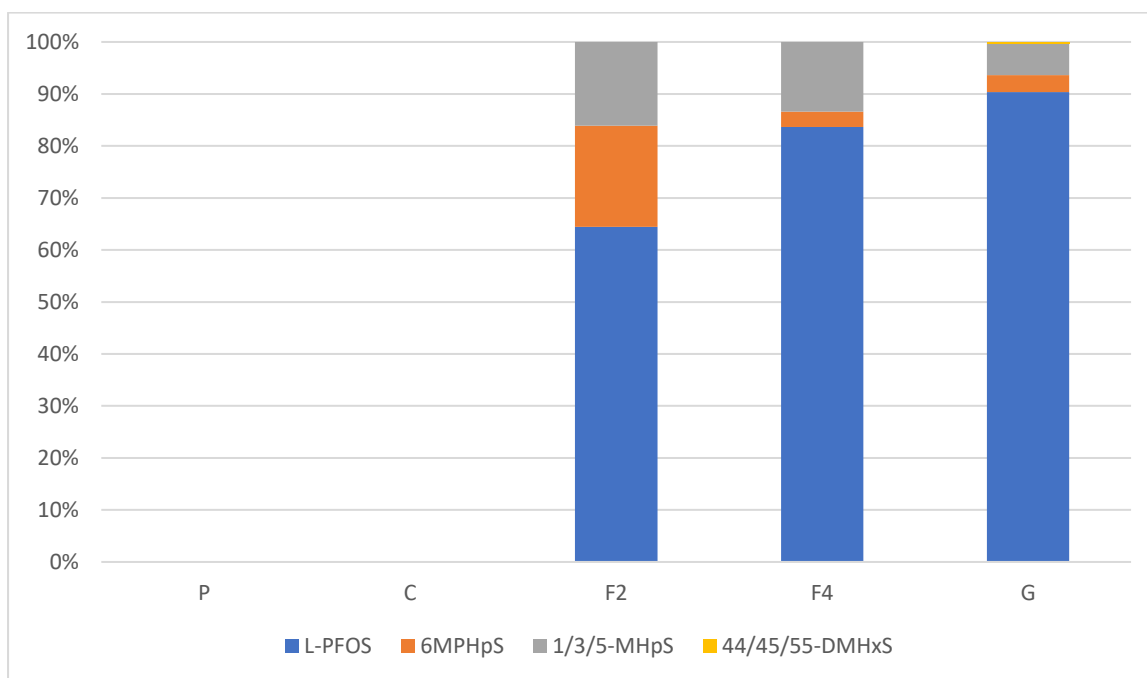


Figure 4-3: Chart overview of the percentage contributions to the PFOS isomer profile from each analyte at the different sample types and stations.

No isomers were detected in the zooplankton and crab samples, making it difficult to comment on the isomer compositions in these samples. A more sensitive method is needed for quantitation of analytes at such low concentrations.

4.3 QA and validation criteria results

Table 5-1 shows an overview of the recoveries calculated from the recovery samples. The recovery ranges were generally 67.0-93.6%, all in the acceptable 40-120% range. Based on the calculations the method was validated with regards to recoveries.

Table 5-1: Calculated recoveries in the different recovery samples.

<i>Analyte</i>	<i>%R Zooplankton</i>	<i>%R Crab</i>	<i>%R Fish liver</i>
<i>L-PFOS</i>	70.2	80.3	84.5
<i>P6MHpS</i>	73.7	67.0	60.7
<i>P1/P3/P5-MHpS</i>	80.0	88.1	75.1
<i>P44/P45/P55</i>	82.3	93.6	85.0

The other calculations of the other validation criteria – linear range, linearity, LODs and LOQs – are presented in table 5-2. The linearity requirements were satisfied for all analytes. The linear range was shorter for L-PFOS, who's signals were weaker at the lower end of the calibration curve, and were therefore excluded. LOD and LOQ values are presented in ng/mL. All individual sample data and concentrations were first checked against these values prior to further data handling. Meaning that the analyte concentrations were converted from ng/mL to µg/kg only after their levels were checked against these limit values.

Table 5-2: Overview over the linear ranges, R^2 -values, LODs and LOQs for the different analytes.

<i>Analyte</i>	<i>Linear range (ng/mL)</i>	<i>R²</i>	<i>LOD (ng/mL)</i>	<i>LOQ (ng/mL)</i>
<i>L-PFOS</i>	0.5-20	0.999	0.2703	0,9011
<i>P6MHpS</i>	0-20	0.995	0.0103	0.0345
<i>P1/P3/P5-MHpS</i>	0-20	0.999	0.0106	0.0355
<i>P44/P45/P55</i>	0-20	0.999	0.0077	0.0257

The blank samples didn't show any signs of contamination or carry-over effect, and were therefore not used in the calculations. This was the case both for the procedural, as well as the instrument blanks. This means that, as far as the method was able to detect, no PFOS contribution came from the reagents, materials or instruments used during this method. This signifies that the standards, reagents and mobile phases were pure and free of PFOS, and that no significant PFOS-contamination took place during the procedure.

5. Discussion

5.1 Chromatographic separation

The separation in the current study ended up only partially separation the PFOS isomers. Individual separation was only achieved for L-PFOS and MP6HsS, while the 6 remaining isomers coeluted in two broad peaks – one for the di-perfluoromethylated isomers and one for the mono-perfluorinated ones. Since the reference study the HPLC separation method was modelled after didn't individually separate all the target isomers either, a complete separation was not realistic.

The reference study did achieve a better separation than the current did, obtaining 6 separate peaks. However, it should be noted that it had 10 target isomers, compared to the current study's 8, meaning that more peaks are the default expectation for the separation. When examining the separation of the 8 target isomers for the current study

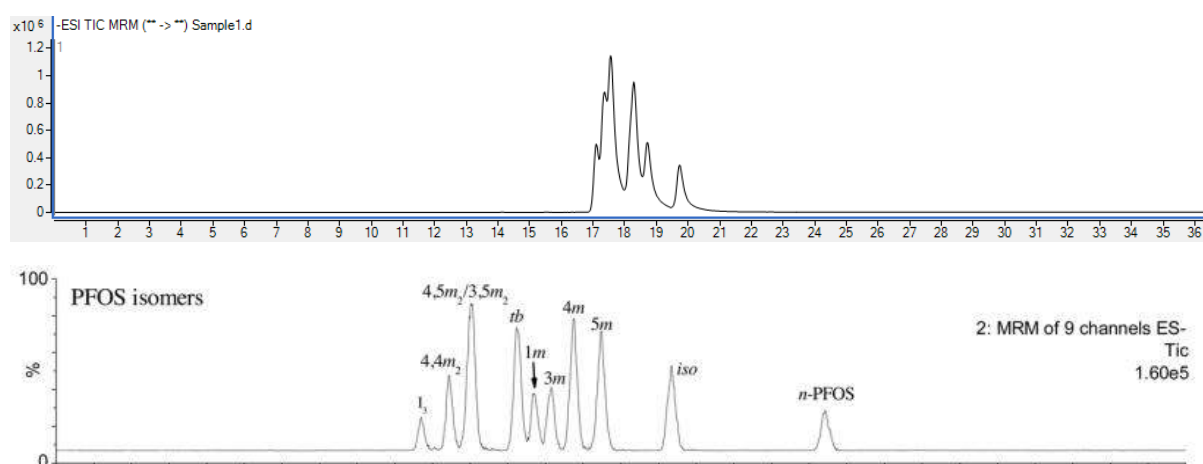


Figure 6-1: Comparisons of the separations achieved in the current study, to the reference study from which the chromatographic method was adapted.

The less successful separation than the reference study was likely a result of the sum of multiple minor differences in method setup, equipment and execution between the studies. The retention times obtained in the current study match those of the reference study, suggesting that there were no issues with the pressure stability or the pump systems. Broader peaks indicate issues with either the injection or the separation. The same chromatographic column being used for both studies points to either insufficient conditioning prior to sample run or damaged stationary phase. The column was carefully handled throughout the procedure and had not been used prior to this study, meaning column damage was unlikely.

Another difference between the methods relates to the injection volumes. Initial standards injection testing was plagued by sensitivity issues, resulting in most of the peaks drowning in noise at concentrations at the lower end of the calibration curve. This was likely due to improper MRM parameter set-up and lack of product ion specific optimisation. It is a commonly known fact that excessive injection volumes tend to cause band broadening in the resulting chromatograms. Although the broadening is highly dependent on specifics such as equipment, analytes and mobile phases, it has been shown that large amounts of analytes can cause wider peaks and worse peak separations (Kozlowski & Dalterio, 2007). This is supported by the observation of significant peak tailing in most of the chromatograms. Tailing is often caused by overloading the column with too large injections. Doubling the injection volume likely increased the signals at the cost of peak separation. Additionally, the other MS parameters were adopted from a reference PFAS study without any changes, although this was a PFOS-isomer method only.

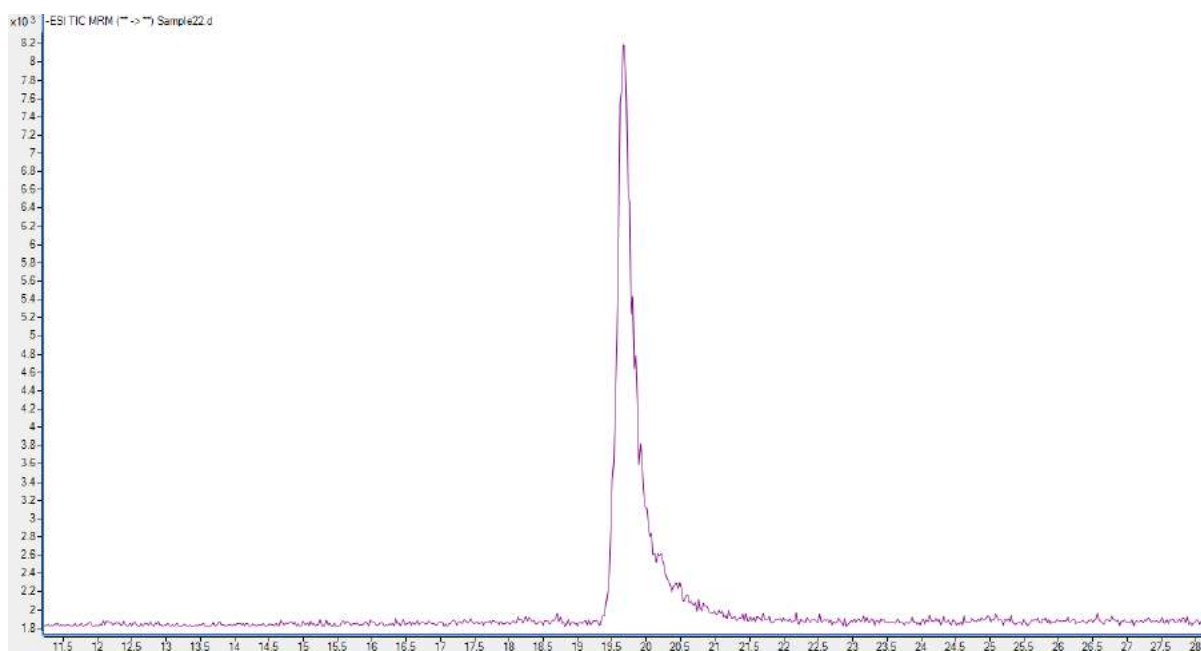


Figure 6-2: The chromatographic peak of 10 μL pure L-PFOS standard injected at 10 ng/mL.

Improving the current method should therefore primarily focus on optimising the MS and MRM parameters for the individual target PFOS isomers and decreasing the injection volume to 5 μL – as opposed to 10 μL . This would likely improve the separation to the extent that was achieved in the reference study.

5.2 Analyte results and findings

As shown in the results section, no PFOS isomers were detected in zooplankton or crab samples. This is likely due to their low concentrations at such low trophic levels. This is in agreement with the reference study conducted on the PFAS levels in Svalbard (Ali et al. 2021), where PFOS levels in zooplankton from station 4 were found to be under 1.0 µg/kg, and thus too low to be quantified with the current method (Ali et al. 2021). PFOS levels in crab samples from station 4 were found to be in concentrations of approximately 0.5 µg/kg.

Apart from the dimethylated isomers, the rest of the PFOS analytes were detected and quantified in fish liver and gull liver samples. Fish from station 4 showed higher PFOS concentrations than fish from station 2, also in agreement with Ali et al. (2021). Gull samples showed very variable levels of total PFOS between the individual samples. This is likely a result of the inconsistent and opportunistic diet of this high trophic level predator in the Arctic.

When it comes to isomer-profiles, sufficient insights were obtained from the fish and gull samples to see general trends in its changes in the higher trophic part of the arctic food web. Since only PFOS isomers from two trophic levels were obtained, conclusions can only be drawn from that transition only, and not about the entire food web as a whole.

What can be observed from the changes in PFOS isomer composition from fish liver to gull liver, is a percentage-wise increase in the presence of L-PFOS compared to the two other monomethylated branched analytes. The L-PFOS contribution was about 90% in the gull samples, while fish liver samples had L-PFOS content corresponding to a range of 65-85%. Both the other analytes decreased percentage-wise going from fish to gull samples.

The dimethylated PFOS analyte was also quantified in gull samples, whereas it was below the detection limits in most fish liver samples. The perceived visual increase of dimethylated PFOS that can be seen in figure x is likely not indicative of some bioaccumulation trend, but rather of that the total PFOS concentrations were so high compared to the other trophic levels, that PDMHxS concentrations too were inflated and finally at concentrations allowing quantification. Meaning that their percentage-wise contribution likely did not increase at all, and probably decreased in reality, like it has been reported to do in previous studies of Br-PFOS in food chains.

There was a significant difference between both the total PFOS levels as well as the isomer profile make-ups of the fish liver samples from the two different sampling stations. The L-PFOS percentage in station 2 was 65%, compared to almost 85% for station 4. This means that the L-PFOS contribution in station 4 was higher than its contribution in technical ECP PFOS product (about 70% L-PFOS), while station 2 had somewhat lower. Ali et al. (2021) also reported higher relative L-PFOS levels in station 4 fish samples, the relative L-PFOS/Br-PFOS ratios were approximately 60% and 70%, respectively at station 2 and 4. A likely explanation for this discrepancy is different individual levels in the selected samples, but even dietary explanations fall short, as it isn't so much the total PFOS concentrations that are surprising, but rather the significant differences in isomer profiles.

L-PFOS has been known to have greater bioaccumulation properties than its branched counterparts. This explains the jump in relative L-PFOS levels seen from fish liver to gull liver samples. But at the same trophic level the only known distinguishing factor between the fish liver samples are the locations at which they were collected. Station 2 is next to the decommissioned FFTS, while station 4 was assumed to not be influenced by known local PFOS sources, reflecting the PFOS levels in the fjord at large.

Multiple studies have reported the faster degradation of branched PFOS isomer precursors in the environment compared to L-PFOS precursors. Elevated Br-PFOS levels, compared to the ECF technical isomer mixture, may indicate this process happening to the point where the L-PFOS concentrations are decreasing compared with Br-PFOS. On the other hand, bioaccumulation must be the main process driving influencing the PFOS isomer profile in the livers of fish at station 2. In addition to greater exposure to ECF products through local pollution sources may counteract the degradation of branched isomers. This could have been a possible explanation, but if station 2 is more exposed to pollution and total PFOS as a consequence of that, then why are the total PFOS levels higher in station 4 samples?

There may be other factors at play that influence the concentrations and isomer profiles presented here. A part of the explanation could lie in the fact that not all ECF PFOS isomers were determined in the current study, resulting in that the sum of the branched isomers was underreported. This could potentially mean that the relative L-PFOS levels should be lower in both fish liver and gull samples. Lack of insight into what extent the unidentified isomers are contributing to levels of PFOS isomers introduces significant uncertainty with regards to the analytes. Some of them are likely to coelute with the other isomers, and inflate the measured values, but this can't be verified without commercially available individual standard for retention time determination, product ion screening and separation testing.

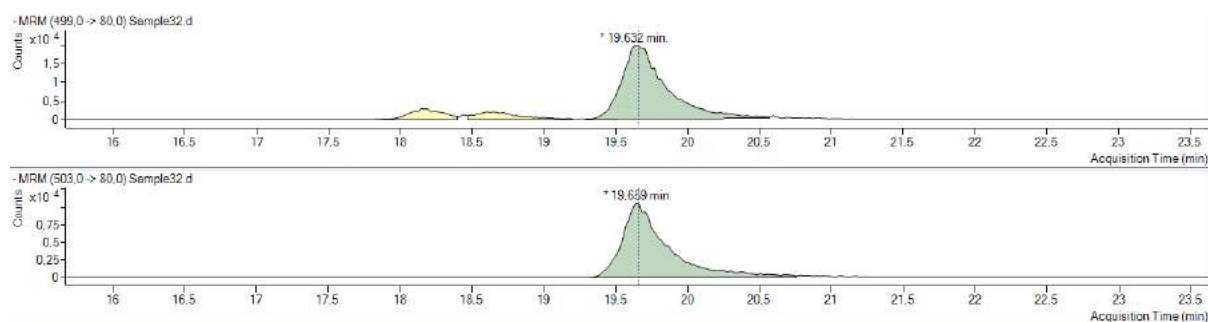


Figure 6-3: The chromatograms of gull liver sample number 85 with the mass transition (499->80). Highlighted here are the peaks of L-PFOS (first chromatogram) and ISTD (second chromatogram).

Furthermore, an increased number of samples from each sample type and each station would be useful to more decrease the uncertainty in the method and ensure more representative data for discussion, and make the conclusions less speculative. Increasing the number of sample types from more trophic levels and stations would also help in creating a more complete picture of the PFOS isomeric differences throughout the food web as well as the fjords surrounding Longyearbyen. More insight into what isomer-profile changes take place at

lower trophic levels could help identify trends that happen at higher ones, as trends are difficult to identify with certainty when only observing changes between two trophic levels.

However, to more detailed information on what happens at the zooplankton and crab level of the food web, more sensitive methods are required. To more easily distinguish analyte signals from noise is integral to obtaining adequate data at a consistent basis. Additionally, better separation is required to elucidate and map out the more isomer-specific trends, rather than analysing the changes that happen to isomers in bulk as they coelute into the same analyte peaks.

Due to limited studies on the PFOS isomer profiles in zooplankton, crabs, fish livers and gull livers in the Arctic, there is little scientific literature to compare the findings with.

Comparison of the L-PFOS/Br-PFOS with previous findings were already done by Ali et al. (2021). At the same time isomer profiles were only quantitated in two trophic levels, making it difficult to identify trends in the isomeric changes in the food web. The quantitation was not isomer-specific for all 8 available standards, and information of the levels and changes in the individual coeluting di- and monomethylated isomers was not obtained. A key take-away is the importance of sensitivity and separation in trace-level environmental HPLC-MS/MS analysis, as well as the interplay between the two.

In the future, it should be a goal to improve the methods separation and the sensitivity. Better separation will as mentioned likely be achieved with reduced injection volumes and better column conditioning. Meanwhile sensitivity can be improved by optimising the MS/MS-parameters by studying the individual isomers fragmentation in response to changes in parameters such as collision energy and exit potential. The results and findings offer promise with respect to the methods future potential improvements and applications.

6. Conclusions

The current study attempted to design a new ESI-HPLC-MS/MS method for the isomer-specific quantitative determination of PFOS isomers at trace levels in a food web in the Norwegian Arctic. A crude separation yielding four distinguishable isomer signals was achieved, and the method was used to explore the isomer profile changes happening at different trophic levels in a food web.

The method was validated and showed good linearity and adequate recoveries in the ranges of 60%-94% in zooplankton, crab and fish liver samples. LOD and LOQ values were significantly higher for L-PFOS than for the remaining analytes, and standard concentrations at the lower end of the calibration curve could not be distinguished from noise.

The method lacked the necessary sensitivity to quantitate isomers at lower trophic levels, thus no new information was gained about the isomer composition changes in the levels between zooplankton and fish. The changes to the isomer profile from fish liver to gull liver was studied, and the total PFOS concentrations as well as the relative levels of L-PFOS were found to increase with increasing trophic levels. Large individual varieties in the levels of PFOS in full livers were in agreement with a reference study examining the same area.

Significant differences in the total PFOS concentrations as well as the relative contributions from different isomers were observed in fish liver samples from a reference station unaffected by local PFOS pollution and a sampling station next to a decommissioned fire-fighting training station. The PFOS concentrations were surprisingly higher at the reference station, and the isomer composition indicated that they were exposed to different PFOS sources.

More samples from multiple trophic levels and locations are needed to examine and identify the trends in isomer profile changes in the arctic food web. In addition, a lack of commercially available individual isomer standards makes it difficult to control for interferences and contributions from the unidentified isomers present in the environmental samples. Significant improvements can be made to the method through MRM-optimisation to increase sensitivity and to the chromatographic separation, to allow for more isomer-selective quantitation, but it was shown that the method can be applied to higher trophic levels in its current form.

7. Future perspectives

The current study has demonstrated the potential of the appliance of ESI-HPLC-MS/MS in the context of isomer-specific environmental trace-analysis. However, adjusting the method design, optimising the MS/MS-parameters and improving the chromatographic separation is likely to greatly improve the methods performance and increase its potential uses. Increased sensitivity will in turn allow for detection of analytes at lower concentrations without the need to overload the column with larger volumes.

Increased blank sample use from the moment the samples are collected can account for pollution throughout the early parts of the sample handling. Matrix matched calibration can be used to more accurately account for the specific influences on the individual isomer analyte signals.

Obtaining pure individual standards of all 11 isomers that have been identified in ECF technical product will allow for better control of potential interferences and contributions to the analyte signals. Slight improvements in these parts of the method can result in a solid and reliable method of isomeric PFOS analysis.

8. References

1. 3MCompany. (1999). Fluorochemical use, distribution and release overview.
2. Ahrens, L., Vorkamp, K., Lepom, P., Theobald, N., Ebinghaus, R., Bossi, R., Barber, J. & McGovern, E. (2010). Determination of perfluoroalkyl compounds in water, sediment, and biota: International Council for the Exploration of the Sea.
3. Ali, A. M., Langberg, H. A., Hale, S. E., Kallenborn, R., Hartz, W. F., Mortensen, Å. K., Ciesielski, T. M., McDonough, C. A., Jenssen, B. M., Breedveld, G. D. (2021) The fate of poly- and perfluoroalkyl substances in a marine food web influenced by land-based sources in the Norwegian Arctic. *Environmental Science: Processes & Impacts*, 23, 588.
4. Armitage JM, Cousins IT, Buck RC, Prevedouros K, Russell MH, MacLeod M, Korzeniowski SH (2006) Modeling global-scale fate and transport of perfluorooctanoate emitted from direct sources. *Environmental Science & Technology*, 40:6969–6975.
5. Buck, R. C., Franklin, J., Berger, U., Conder, J. M., Cousins, I. T., de Voogt, P., Jensen, A. A., Kannan, K., Mabury, S. A. & van Leeuwen, S. P. (2011). Perfluoroalkyl and polyfluoroalkyl substances in the environment: terminology, classification, and origins. *Integr Environ Assess Manag*, 7 (4): 513-41.
6. Chu, S. & Letcher, R. J. (2009). Linear and branched Perfluorooctane Sulfonate Isomers in Technical Product and Environmental Samples by In-Port Derivatization-Gas Chromatography-Mass Spectrometry. *Analytical Chemistry* 2009 81 (11), 4256-4262. Available from: doi 10.1021/ac8027273 [Accessed 6 September 2021].
7. Conder, J. M., Hoke, R. A., De Wolf, W., Russell, M. H. & Buck, R. C. (2008). Are PFCAs bioaccumulative? A critical review and comparison with regulatory lipophilic compounds. *Environmental Science & Technology*, 42 (4): 995-1003
8. De Silva AO, Mabury SA (2004) Isolating isomers of perfluorocarboxylates in polar bears (*Ursus maritimus*) from two geographical locations. *Environmental Science & Technology*. 38:6538–6545.
9. De Silva AO (2010) Isomer profiling of perfluorinated substances as a tool for source tracking: a review of early findings and future applications. *Environmental Contamination and Toxicology*. 208:111-60.
10. Dietz, R., Bossi, R., Riget, F. F., Sonne, C. & Born, E. (2008). Increasing perfluoroalkyl contaminants in east Greenland polar bears (*Ursus maritimus*): a new toxic threat to the Arctic bears. *Environmental Science & Technology*, 42 (7): 2701-2707.
11. Ellis DA, Martin JW, Mabury SA, Hurley MD, Andersen MP, Wallington TJ (2003a) Atmospheric lifetime of fluorotelomer alcohols. *Environmental Science & Technology*, 37:3816–3820.

12. Greaves, A. K., Letcher, R. J., Sonne, C., Dietz, R., Born, E. W. (2012). Tissue-Specific Concentrations and Patterns of Perfluoroalkyl Carboxylates and Sulfonates in East Greenland Polar Bears. *Environmental Science & Technology*, 46 (21), 11575-11583.
13. Hanssen, L., Dudarev, A. A., Huber, S., Odland, J. O., Nieboer, E., Sandanger, T. M. (2013). Partition of perfluoroalkyl substances (PFASs) in whole blood and plasma, assessed in maternal and umbilical cord samples from inhabitants of arctic Russia and Uzbekistan. *Science of The Total Environment*, Vol. 447, 1: 430-437.
14. Fang, S., Zhang, Y., Zhao, S., Qiang, L., Chen, M., Zhu, L. (2016). Bioaccumulation of perfluoroalkyl acids including the isomers of perfluorooctane sulfonate in carp (*Cyprinus carpio*) in a sediment/water microcosm. *Environmental Toxicology and Chemistry*, 35 (2): 3005-3013.
15. Frank, H., Christoph, E. H., Holm-Hansen, O. & Bullister, J. L. (2002). Trifluoroacetate in ocean waters. *Environmental science & technology*, 36 (1): 12-15.
16. Giesy, J. P. & Kannan, K. (2001). Global distribution of perfluorooctane sulfonate in wildlife. *Environmental science & technology*, 35 (7): 1339-1342.
17. Houde, M., Czub, G., Small, J. M., Backus, S., Wang, X., Alae, M., Muir, D. C. G. (2008) Fractionation and Bioaccumulation of Perfluorooctane Sulfonate (PFOS) Isomers in a Lake Ontario Food Web. *Environmental Science & Technology*, 42 (24): 9397-9403.
18. Kissa, E. (1994). *Fluorinated Surfactants; Synthesis, Properties, Applications*. Surfactant science series, b. 50. New York: Marcel Dekker, Inc. 469 s
19. Kissa, E. (2001). *Fluorinated surfactants and repellents*. 2nd, Revised and expanded ed. Surfactant science series, b. 97. New York, USA: Marcel Dekker, Inc. 615 s.
20. Kissa E (2005) *Fluorinated surfactants and repellents*, 2nd edn. Marcel Dekker, New York.
21. Kozłowski, E. S., Dalterio, R. A. (2007). Analyte solvent and injection volume as variables affecting method development in semipreparative reversed-phase liquid chromatography. *Journal of Separation Science*. 30 (14): 2286-2292.
22. Kwok, K. Y., Yamazaki, E., Yamashita, N., Taniyasu, S., Murphy, M. B., Horii, Y., Petrick, G., Kallerborn, R., Kannan, K., Murano, K., et al. (2013). Transport of Perfluoroalkyl substances (PFAS) from an arctic glacier to downstream locations: Implications for sources. *Science of The Total Environment*, 447 (0): 46-55.
23. Langois, I., Karmann, A., Van Bavel, B., Lindstrom, G., Oehme, M. (2007). Identification and pattern of perfluorooctane sulfonate (PFOS) isomers in human serum and plasma. *Environment International*, 33:6. 782-788.
24. Moody, C. A. & Field, J. A. (2000). Perfluorinated Surfactants and the Environmental Implications of Their Use in Fire-Fighting Foams. *Environmental Science & Technology*, 34 (18): 3864-3870

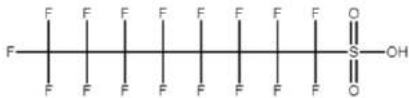
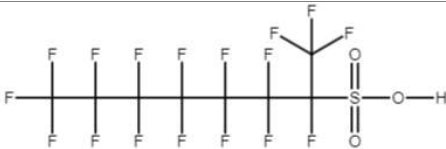
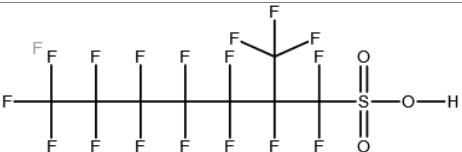
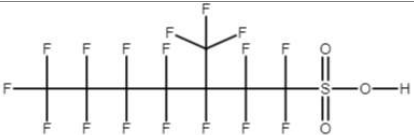
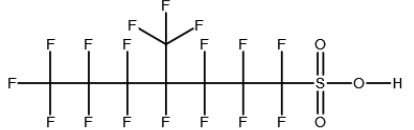
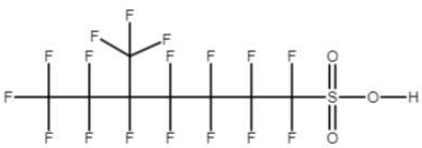
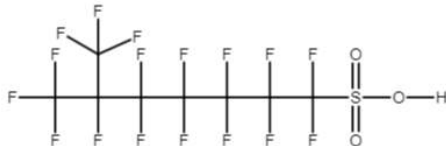
25. Parsons, J. R., Saez, M., Dolfing, J. & de Voogt, P. (2008). Biodegradation of Perfluorinated Compounds. *Reviews of Environmental Contamination and Toxicology*, Vol 196: 53-71.
26. Paul AG, Jones KC, Sweetman AJ (2009) A first global production, emission, and environmental inventory for perfluorooctane sulfonate. *Environmental Science & Technology* 43:386–392.
27. Place, B. J. & Field, J. A. (2012). Identification of Novel Fluorochemicals in Aqueous Film-Forming Foams Used by the US Military. *Environmental Science & Technology*, 46 (13): 7120-7127.
28. Post, G. B., Cohn, P. D. & Cooper, K. R. (2012). Perfluorooctanoic acid (PFOA), an emerging drinking water contaminant: a critical review of recent literature. *Environmental research*, 116: 93-117.
29. Prevedouros, K., Cousins, I. T., Buck, R. C. & Korzeniowski, S. H. (2006). Sources, fate and transport of perfluorocarboxylates. *Environmental Science & Technology*, 40 (1): 32-44.
30. Sanderson, H., Boudreau, T. M., Mabury, S. A., Cheong, W. J., Solomon, K. (2009). Ecological impact and environmental fate of perfluorooctane sulfonate on the zooplankton community in indoor microcosms. *Environmental Toxicology*, Vol. 21 (7): 1490-1496.
31. Shoeib, M., Harner, T. & Vlahos, P. (2006). Perfluorinated Chemicals in the Arctic Atmosphere. *Environmental Science & Technology*, 40 (24): 7577-7583
32. Smart, B. E. (2001). Fluorine substituent effects (on bioactivity). *Journal of Fluorine Chemistry*, 109 (1): 3-11.
33. Skaar, J. S., Ræder, E. M., Lyche, J. L., Ahrens, L., Kallenborn, R. (2019). Elucidation of contamination sources for poly- and perfluoroalkyl substances (PFASs) on Svalbard (Norwegian Arctic). *Environmental Science & Pollution Research* 26, 7356–7363.
34. Sturm, R. & Ahrens, L. (2010). Trends of polyfluoroalkyl compounds in marine biota and in humans. *Environmental Chemistry*, 7 (6): 457-484.
35. Tomy, G. T., Budakowski, W., Halldorson, T., Helm, P. A., Stern, G.A., Friesen, K., Pepper, K., Tittlemier, S. A., Fisk, A. T. (2004). Fluorinated Organic Compounds in an Eastern Arctic Marine Food Web. *Environmental Science & Technology*, 38 (24), 6475-6481.
36. UNEP. (2009). Governments unite to step-up reduction on global DDT reliance and add nine new chemicals under international treaty. Geneva: Secretariat of the Stockholm Convention.
37. Vyas SM, Kania-Korwel I, Lehmler HJ (2007) Differences in the isomer composition of perfluorooctanesulfonyl (PFOS) derivatives. *J Environ Sci Health A Tox Hazard Subst Environ Eng*. 42:249–255.

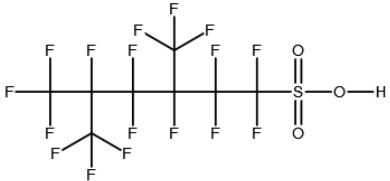
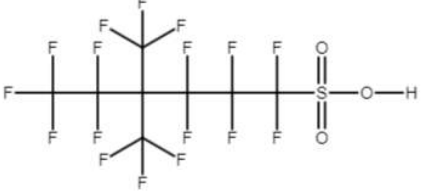
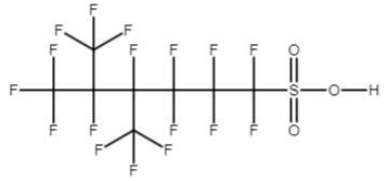
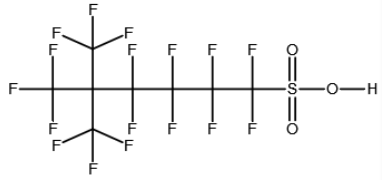
38. Wang, Z., Cousins, I. T., Scheringer, M. & Hungerbühler, K. (2013). Fluorinated alternatives to long-chain perfluoroalkyl carboxylic acids (PFCAs), perfluoroalkane sulfonic acids (PFSA) and their potential precursors. *Environment International*, 60 (0): 242-248.
39. Wang, J., Zheng, X. W., Bloom, M. S., Qian, Z., Hinyard, L. J. (2019). Renal function and isomers of perfluorooctanoate (PFOA) and perfluorooctanesulfonate (PFOS): Isomers of C8 Health Project in China. *Chemosphere*. 218: 1042-1049.
40. Wania F (2007) A global mass balance analysis of the source of perfluorocarboxylic acids in the Arctic Ocean. *Environmental Science & Technology*, 41:4529–4535.
41. Young CJ, Furdui VI, Franklin J, Koerner RM, Muir DC, Mabury SA (2007) Perfluorinated acids in Arctic snow: new evidence for atmospheric formation. *Environmental Science & Technology*, 41:3455–3461.
42. Zhang, H., Wen, B., Wen, W., Ma, Y., Hu, X., Wu, Y., Luo, L, Zhang, S. (2017). Determination of perfluoroalkyl acid isomers in biosolids, biosolids-amended soils and plants using ultra-high performance liquid chromatography tandem mass spectrometry. *Journal of Chromatography B*, 1072 25-33.

9. Appendix

Appendix A – Chemicals

Table A-1: Terminology, acronyms and chemical structures of the 11 PFOS isomers present in T-PFOS.

Name	Acronym	Chemical structure (protonated)
Perfluorooctanesulfonic acid	L-PFOS	
Perfluoro-1-methylheptane sulfonic acid	P1MHpS	
Perfluoro-2-methylheptane sulfonic acid	P2MHpS	
Perfluoro-3-methylheptane sulfonic acid	P3MHpS	
Perfluoro-4-methylheptane sulfonic acid	P4MHpS	
Perfluoro-5-methylheptane sulfonic acid	P5MHpS	
Perfluoro-6-methylheptane sulfonic acid	P6MHpS	
Perfluoro-3,5-dimethylhexane sulfonic acid	P35DMHxS	

		
Perfluoro-4,4-dimethylhexane sulfonic acid	P44DMHxS	
Perfluoro-4,5-dimethylhexane sulfonic acid	P45DMHxS	
Perfluoro-5,5-dimethylhexane sulfonic acid	P55DMHxS	

Appendix B – Standards, reagents and materials

Table B.1: Complete list of chemicals.

Full name	CAS-number	Supplier	Purity %	Size	Use
Acetonitrile	75-05-8	Merck, Germany		1.0 L	Solvent in extraction
Ammonium acetate	631-61-8	Sigma-Aldrich, USA	99.99	1.0 kg	Buffer solutions during extraction,
Ammonium formate	540-69-2	Sigma-Aldrich, USA	97	500 g	Mobile phase
Ammonium hydroxide 25%	1336-21-6	Merck, Germany	25%	500 mL	Solvent during extraction

ENVI-carb	-	Sigma-Aldrich, USA	-	50 g	Clean-up following extraction
70% Ethanol	64-17-5	Sigma-Aldrich, USA	Reagent grade	250 mL	
Methanol	HiPerSolv	VWR, Norway	99.9	2.5 L	Solvent
Methanol	67-56-1	Sigma-Aldrich, USA	>99.8	2.5 L	Mobile phase

Table B-2: Complete list of standards.

Name	Acronym	Cas number	Supplier	Purity
Sodium perfluoro-1-[1,2,3,4-13C4] octanesulfonate	MPFOS	960315-53-1	Wellington Laboratories	>99%
Sodium perfluoro-1-octanesulfonate	L-PFOS	4021-47-0	Wellington Laboratories	>99%
Perfluoro-1-methylheptane sulfonate	P1MHpS	N/A	Wellington Laboratories	>99%
Perfluoro-2-methylheptane sulfonic acid	P2MHpS	N/A	Wellington Laboratories	>99%
Perfluoro-3-methylheptane sulfonic acid	P3MHpS	N/A	Wellington Laboratories	>99%
Perfluoro-4-methylheptane sulfonic acid	P4MHpS	N/A	Wellington Laboratories	>99%
Perfluoro-5-methylheptane sulfonic acid	P5MHpS	N/A	Wellington Laboratories	>99%
Perfluoro-6-methylheptane sulfonic acid	P6MHpS	N/A	Wellington Laboratories	>99%
Perfluoro-3,5-dimethylhexane sulfonic acid	P35DMHxS	N/A	Wellington Laboratories	>99%
Perfluoro-4,4-dimethylhexane sulfonic acid	P44DMHxS	N/A	Wellington Laboratories	>99%
Perfluoro-4,5-dimethylhexane sulfonic acid	P45DMHxS	N/A	Wellington Laboratories	>99%

Perfluoro-5,5-dimethylhexane sulfonic acid	P55DMHxS	N/A	Wellington Laboratories	>99%
--	----------	-----	-------------------------	------

Table B-3: Complete list of materials and consumables.

Name	Supplier
Nitrile green gloves	VWR International AS
Nitrile blue gloves	VWR International AS
Oasis WAX 6cc 500 mg	Waters, USA
Pasteur pipettes	VWR International AS
Polypropylene vials, 1.5 mL	VWR International
Spin-X centrifuge tube filters	Costar, Corning, NY, USA
Proline Automatic pipette 5-50 μ L	Biohit, Helsinki, Finland
Proline Automatic pipette 10-100 μ L	Biohit, Helsinki, Finland
Proline Automatic pipette 100-1000 μ L	Biohit, Helsinki, Finland

Table B-4: Complete list of instruments.

Name	Producer	Description
Agilent 1200 Series UPLC system	Agilent Technologies, Santa Clara, CA, USA	
6400 Series Triple Quadrupole LC/MS	Agilent Technologies, Santa Clara, CA, USA	
Agilent 1200 Series High Performance Autosampler	Agilent Technologies, Santa Clara, CA, USA	
Agilent 1200 Series Binary Pump	Agilent Technologies, Santa Clara, CA, USA	
Agilent 1200 Series Column Compartment	Agilent Technologies, Santa Clara, CA, USA	
Masshunter Workstation software: Quantitative analysis for QQQ	Agilent Technologies, Santa Clara, CA, USA	SW version B.10.01
MassHunter Workstation Software: Qualitative analysis for QQQ version B.06.00 / Build 6.0.633.10	Agilent Technologies, Santa Clara, CA, USA	SW version B.10.01
Vacuum manifold	Agilent technologies	
Epic FO LB Chromatography column (1.8 μm , 120 \AA , 2.1 mm \times 150 mm)	ES Industries	Perfluorinated C8 column
Centrifuge 5430 R	Eppendorf, Hamburg, Germany	
Analytical scale XP204 (max. 220 g, d = 0.1 mg)	Greifensee, Switzerland	
N-EVAP 111 OA Heat Analytical Nitrogen Evaporator	Organomation, Berlin, MA, USA	
Ultrasonic Cleaner USC600T	VWR International, Leuven, Belgium	
Vortex mixer	VWR International AS, Oslo, Norway	

Appendix C – Instrumental parameters

MS QQQ Mass Spectrometer

Ion Source	AJS ESI	Tune File	D:\MassHunter\Tune\QQQ\G6460A \atunes.TUNE.XML
Stop Mode	By StopTime	Stop Time (min)	45
Time Filter	Off	Time Filter Width (min)	0.07

Time Segments

Index	Start Time (min)	Scan Type	Ion Mode	Div Valve	Delta EMV (-)	Store
1	0	MRM	ESI+Agilent Jet Stream	To MS	400	Yes

Source Parameters

Parameter	Value (+)	Value (-)
Gas Temp (°C)	300	300
Gas Flow (l/min)	5	5
Nebulizer (psi)	25	25
SheathGasHeater	350	350
SheathGasFlow	11	11
Capillary (V)	2000	2500
VCharging	2000	500

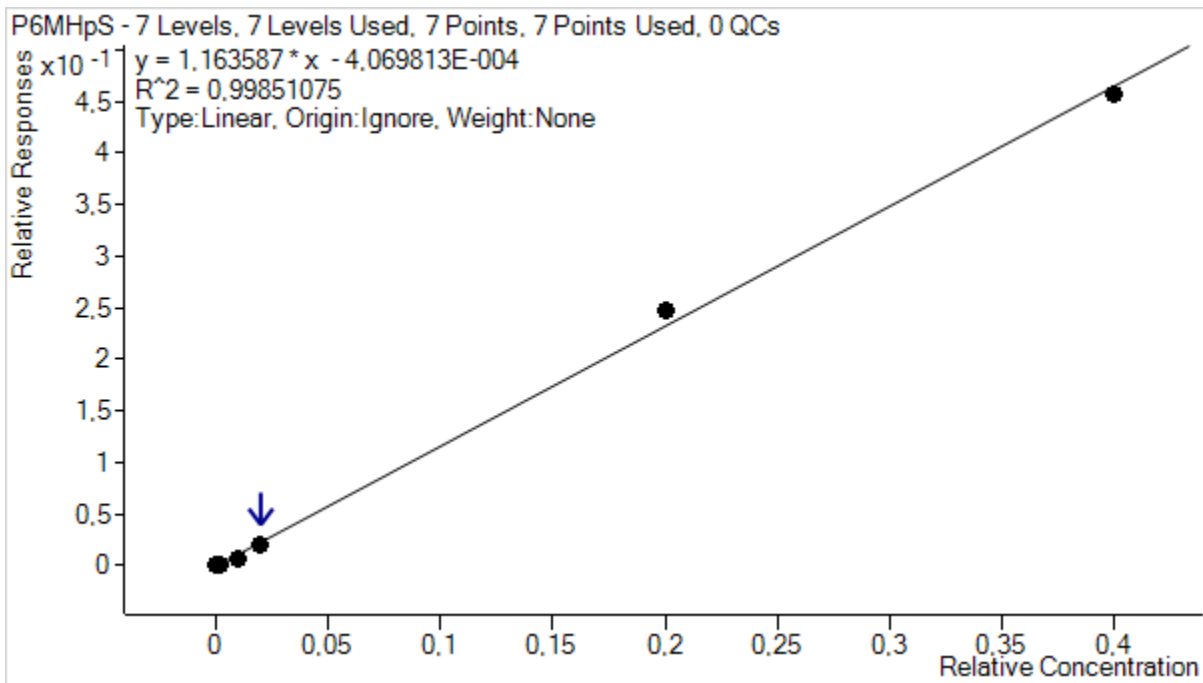
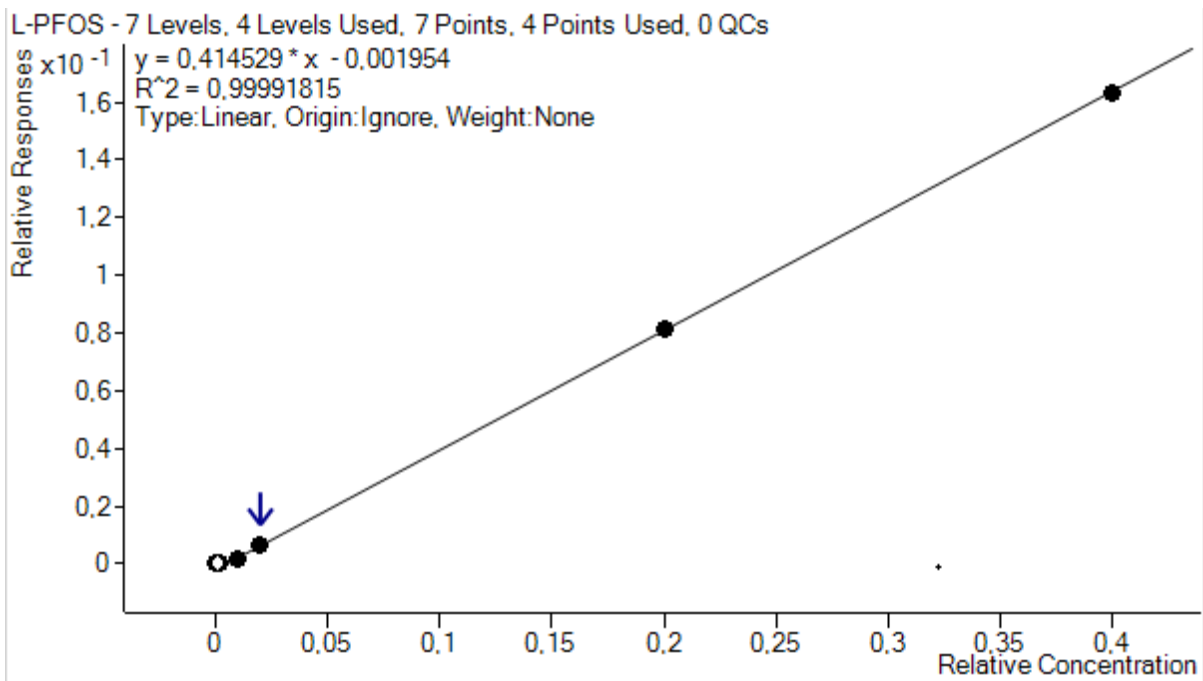
Cpd Group	Cpd Name	ISTD?	Prec Ion	MS1 Res	Prod Ion	MS2 Res	Dwell	Frag (V)	CE (V)	Cell Acc (V)	Polarity
	MPFOS	Yes	503	Unit/Enh (6490)	99	Unit/Enh (6490)	30	200	61	6	Negative
	MPFOS	Yes	503	Unit/Enh (6490)	80	Unit/Enh (6490)	30	200	61	6	Negative
	PFOS	No	499	Unit/Enh (6490)	419	Unit/Enh (6490)	30	200	61	6	Negative
	P45DMHx S	No	499	Unit/Enh (6490)	330	Unit/Enh (6490)	30	200	61	6	Negative
	P44DMHx S	No	499	Unit/Enh (6490)	330	Unit/Enh (6490)	30	200	61	6	Negative
	PFOS	No	499	Unit/Enh (6490)	330	Unit/Enh (6490)	30	200	61	6	Negative
	P55DMHx S	No	499	Unit/Enh (6490)	320	Unit/Enh (6490)	30	200	61	6	Negative
	P45DMHx S	No	499	Unit/Enh (6490)	230	Unit/Enh (6490)	30	200	61	6	Negative
	P44DMHx S	No	499	Unit/Enh (6490)	230	Unit/Enh (6490)	30	200	61	6	Negative
	P6MHPs	No	499	Unit/Enh (6490)	230	Unit/Enh (6490)	30	200	61	6	Negative
	PFOS	No	499	Unit/Enh (6490)	230	Unit/Enh (6490)	30	200	61	6	Negative
	P55DMHx S	No	499	Unit/Enh (6490)	219	Unit/Enh (6490)	30	200	61	6	Negative
	P5MHPs	No	499	Unit/Enh (6490)	219	Unit/Enh (6490)	30	200	61	6	Negative
	P1MHPs	No	499	Unit/Enh (6490)	219	Unit/Enh (6490)	30	200	61	6	Negative
	PFOS	No	499	Unit/Enh (6490)	219	Unit/Enh (6490)	30	200	61	6	Negative
	P6MHPs	No	499	Unit/Enh (6490)	169	Unit/Enh (6490)	30	200	61	6	Negative
	P1MHPs	No	499	Unit/Enh (6490)	169	Unit/Enh (6490)	30	200	61	6	Negative
	L-PFOS	No	499	Unit/Enh (6490)	169	Unit/Enh (6490)	30	200	61	6	Negative
	PFOS	No	499	Unit/Enh (6490)	169	Unit/Enh (6490)	30	200	61	6	Negative
	P45DMHx S	No	499	Unit/Enh (6490)	130	Unit/Enh (6490)	30	200	61	6	Negative
	P44DMHx S	No	499	Unit/Enh (6490)	130	Unit/Enh (6490)	30	200	61	6	Negative
	P5MHPs	No	499	Unit/Enh (6490)	130	Unit/Enh (6490)	30	200	61	6	Negative
	P3MHPs	No	499	Unit/Enh (6490)	130	Unit/Enh (6490)	30	200	61	6	Negative
	PFOS	No	499	Unit/Enh (6490)	130	Unit/Enh (6490)	30	200	61	6	Negative
	PFOS	No	499	Unit/Enh (6490)	119	Unit/Enh (6490)	30	200	61	6	Negative
	P6MHPs	No	499	Unit/Enh (6490)	99	Unit/Enh (6490)	30	200	61	6	Negative
	P3MHPs	No	499	Unit/Enh (6490)	99	Unit/Enh (6490)	30	200	61	6	Negative
	P1MHPs	No	499	Unit/Enh (6490)	99	Unit/Enh (6490)	30	200	61	6	Negative
	L-PFOS	No	499	Unit/Enh (6490)	99	Unit/Enh (6490)	30	200	61	6	Negative
	PFOS	No	499	Unit/Enh (6490)	99	Unit/Enh (6490)	30	200	61	6	Negative
	P55DMHx S	No	499	Unit/Enh (6490)	80	Unit/Enh (6490)	30	200	61	6	Negative
	P45DMHx S	No	499	Unit/Enh (6490)	80	Unit/Enh (6490)	30	200	61	6	Negative
	P44DMHx S	No	499	Unit/Enh (6490)	80	Unit/Enh (6490)	30	200	61	6	Negative
	P6MHPs	No	499	Unit/Enh (6490)	80	Unit/Enh (6490)	30	200	61	6	Negative
	P5MHPs	No	499	Unit/Enh (6490)	80	Unit/Enh (6490)	30	200	61	6	Negative
	P3MHPs	No	499	Unit/Enh (6490)	80	Unit/Enh (6490)	30	200	61	6	Negative
	L-PFOS	No	499	Unit/Enh (6490)	80	Unit/Enh (6490)	30	200	61	6	Negative

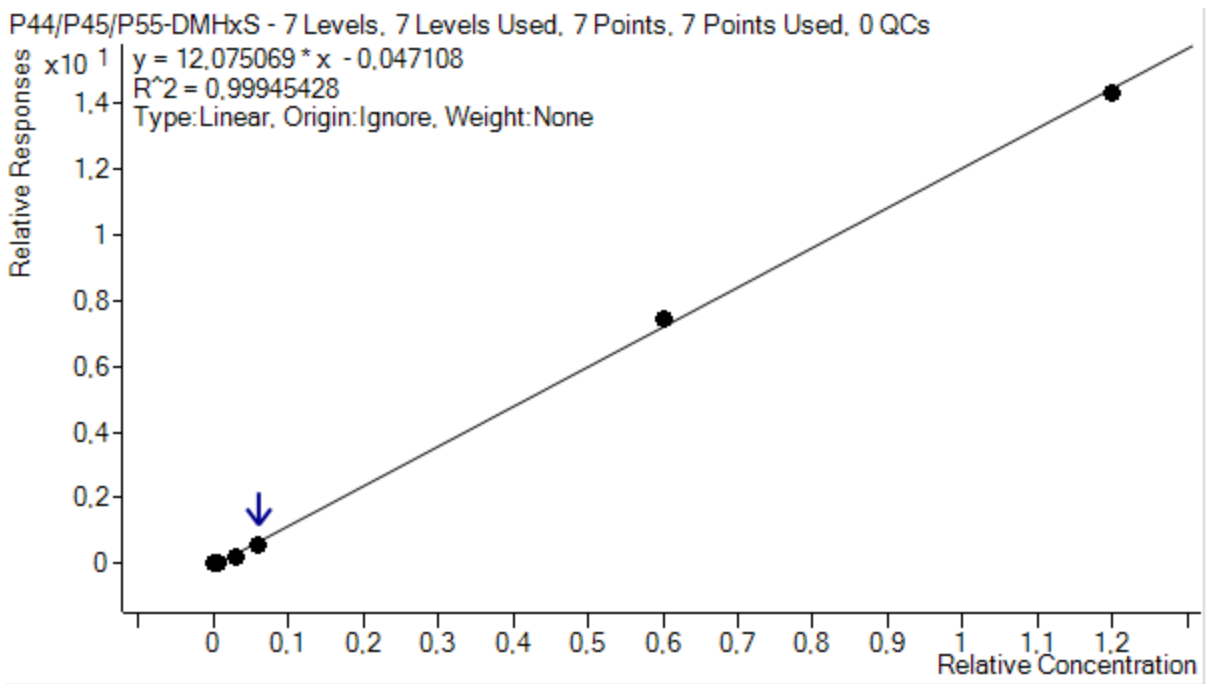
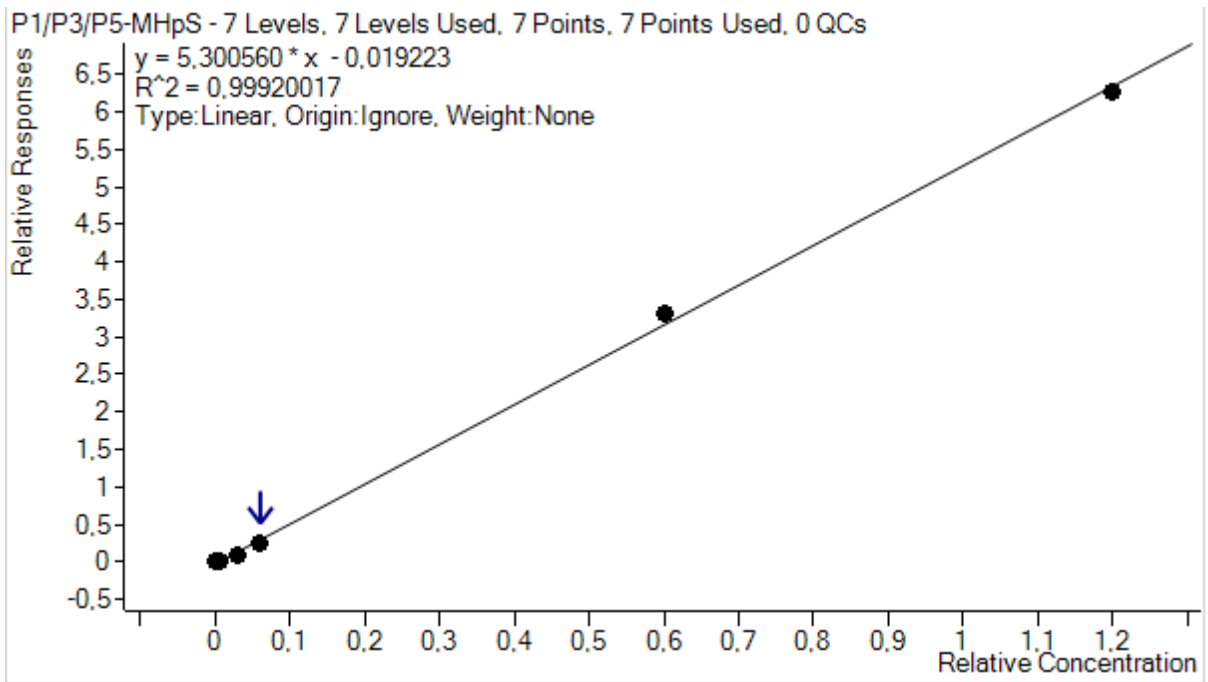
Name:	HiP Sampler	Model:	G1367C
Auxiliary			
Draw Speed		200.0 µL/min	
Eject Speed		200.0 µL/min	
Draw Position Offset		0.0 mm	
Wait Time After Drawing		0.0 s	
Sample Flush Out Factor		5.0	
Vial/Well bottom sensing		No	
Injection			
Injection Mode		Injection with needle wash	
Injection Volume		10.00 µL	
Needle Wash			
Needle Wash Location		Flush Port	
Wash Time		5.0 s	
High throughput			
Automatic Delay Volume Reduction		No	
Overlapped Injection			
Enable Overlapped Injection		No	
Valve Switching			
Valve Movements		1	
Valve Switch Time 1			
Switch Time 1 Enabled		No	
Valve Switch Time 2			
Switch Time 2 Enabled		No	
Valve Switch Time 3			
Switch Time 3 Enabled		No	
Valve Switch Time 4			
Switch Time 4 Enabled		No	
Stop Time			
Stoptime Mode		Time set	
Stoptime		45.00 min	
Post Time			
Posttime Mode		Off	

Name:	Column Comp.	Model:	G1316B
Valve Position		Position 1 (Port 1 -> 2)	
Left Temperature Control			
Temperature Control Mode		Temperature Set	
Temperature		40.0 °C	
Enable Analysis Left Temperature			
Enable Analysis Left Temperature On		Yes	
Enable Analysis Left Temperature Value		0.8 °C	
Right Temperature Control			
Right temperature Control Mode		Temperature Set	
Right temperature		40.0 °C	
Enable Analysis Right Temperature			
Enable Analysis Right Temperature On		Yes	
Enable Analysis Right Temperature Value		0.8 °C	
Stop Time			
Stoptime Mode		Time set	
Stoptime		45.00 min	
Post Time			
Posttime Mode		Off	
Timetable			

Appendix D – Calibration curves

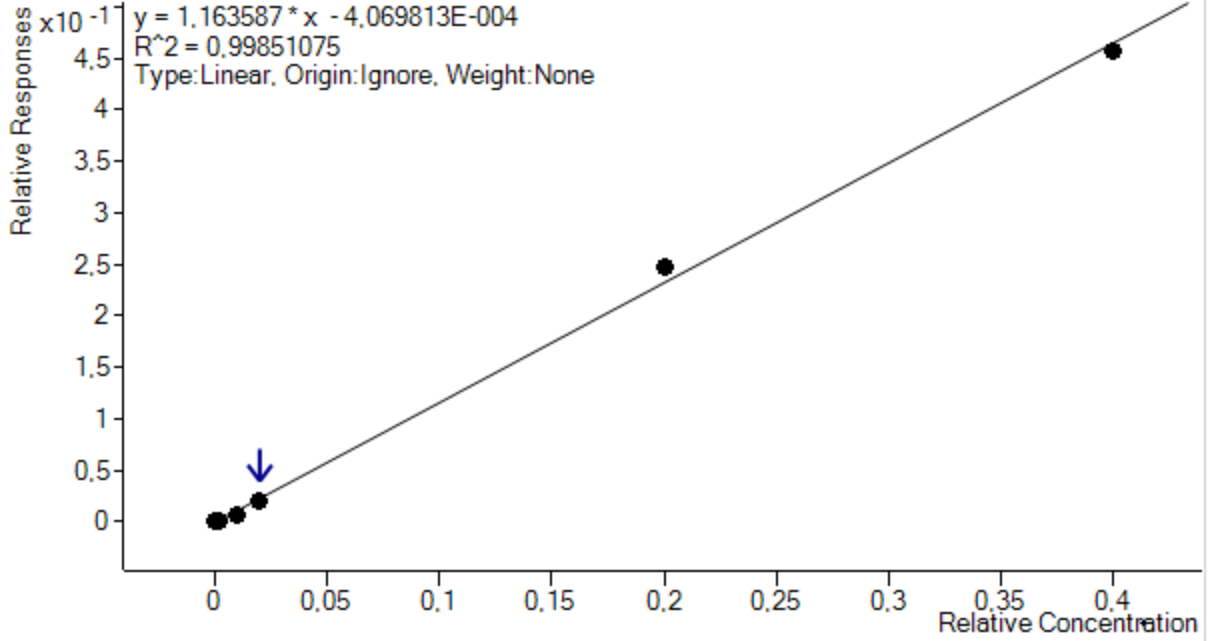
D1 – ISTD method calibration curves



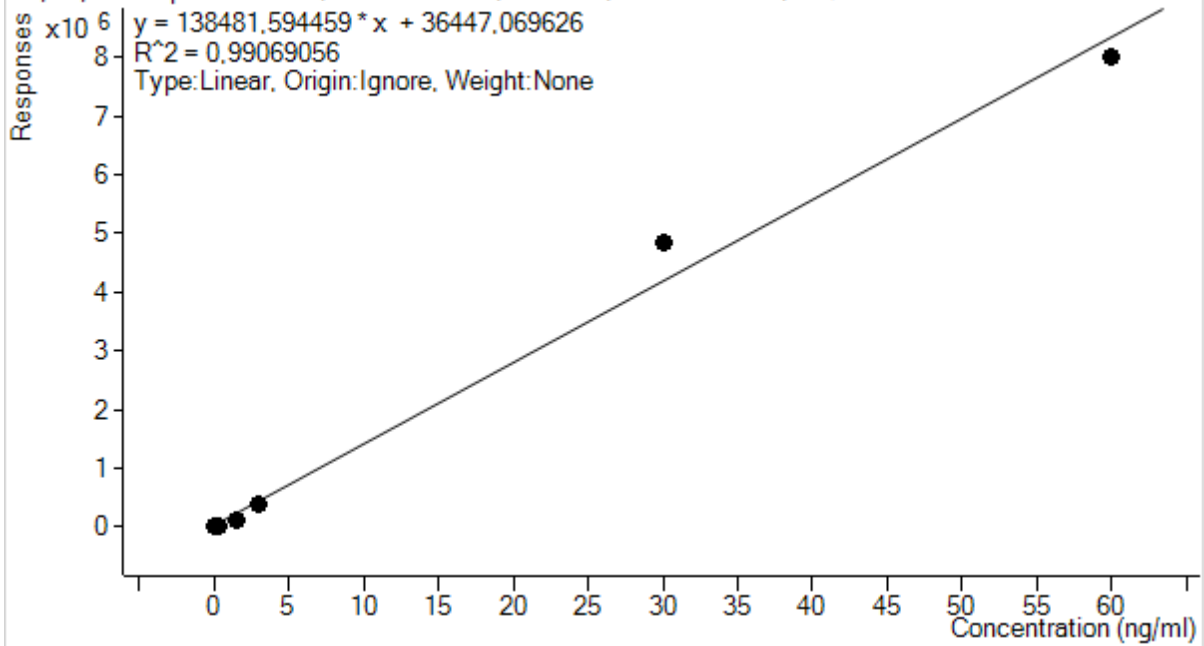


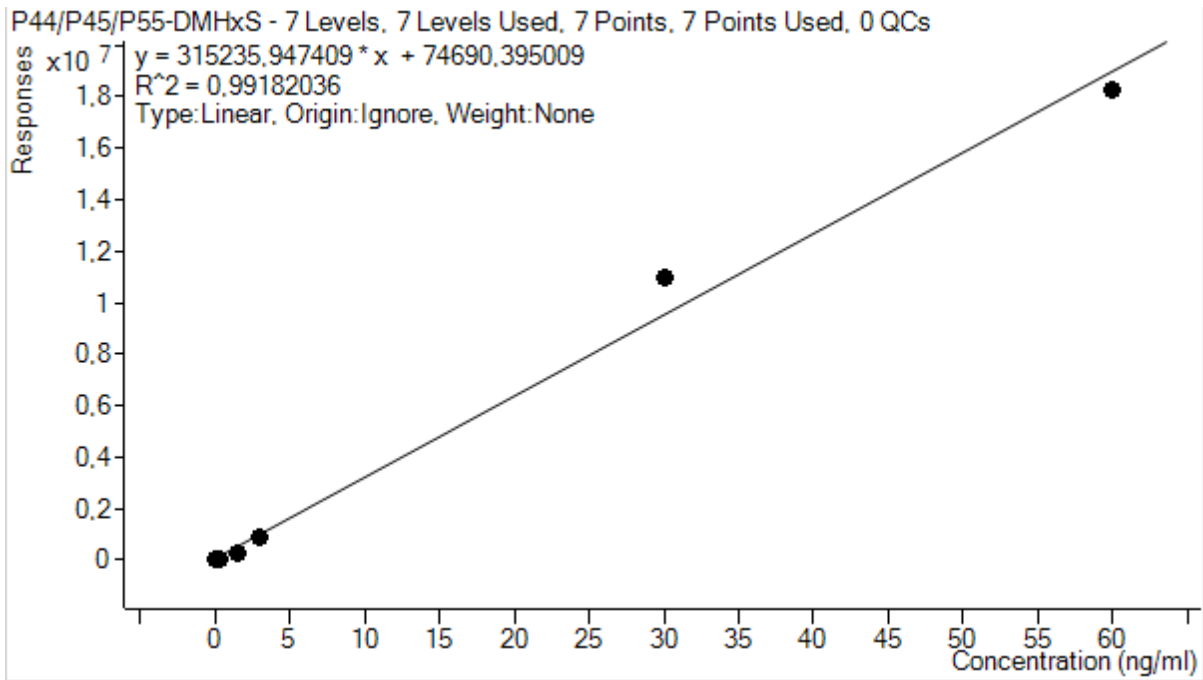
D2 – Calibration curves for LOD and LOQ calculations

P6MHpS - 7 Levels, 7 Levels Used, 7 Points, 7 Points Used, 0 QCs



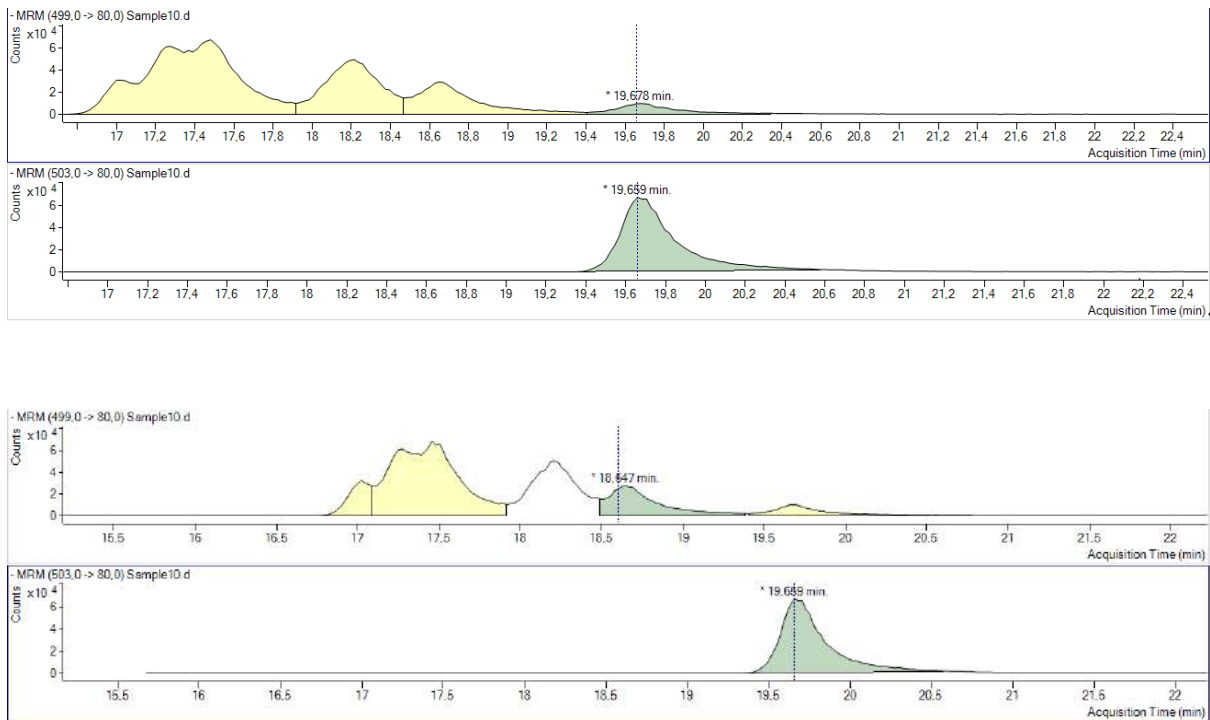
P1/P3/P5-MHpS - 7 Levels, 7 Levels Used, 7 Points, 7 Points Used, 0 QCs

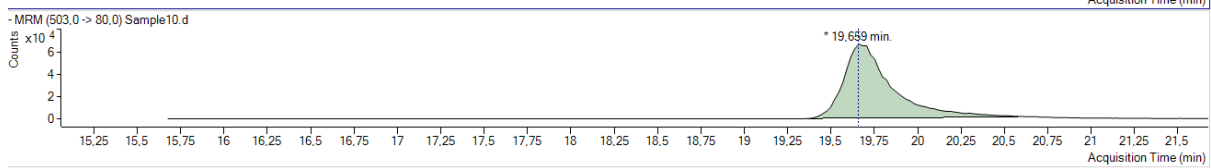
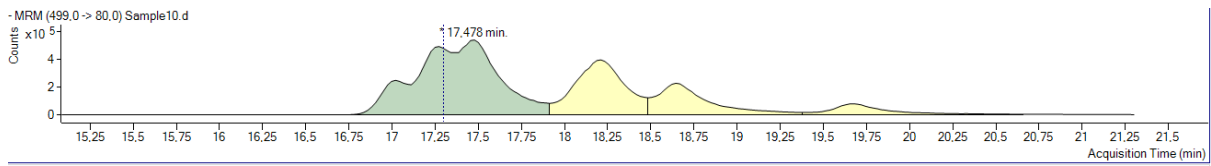
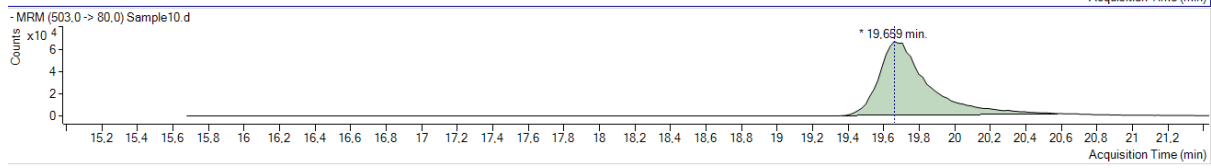
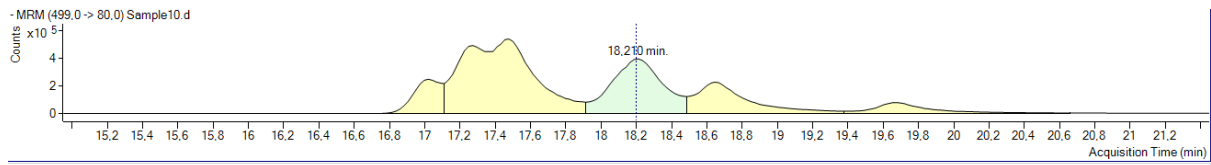




Appendix E - Chromatograms

Examples of some of the chromatograms obtained during the analysis.





Appendix F – Results and validation parameters

Table F-1: Raw data obtained from the quantification of L-PFOS in the samples. Concentrations above LOQ are highlighted as green. Concentrations above LOD are highlighted as orange, and concentrations below LOD are highlighted as red.

Sample				L-PFOS Method					L-PFOS Results				
	Name	Data File	Type	Level	Acq. Date-Time	Exp. Conc.	RT	Resp.	M I	Calc. Conc.	Final Conc.	Accuracy	S/N
	Blank1	Sample 2.d	Sample		11.10.2021 14:31		19,4 49	0	#				
	Blank2	Sample 3.d	Sample		11.10.2021 15:17		19,6 55	0	#				
	0	Sample 4.d	Cal	1	11.10.2021 16:03	0	19,6 55	0	#				
	0.05	Sample 5.d	Cal	2	11.10.2021 16:48	0,05	19,6 55	0	#				
	0.1	Sample 6.d	Cal	3	11.10.2021 17:34	0,1	19,7 01	0	#				
	0.5	Sample 7.d	Cal	4	11.10.2021 18:20	0,5	19,6 78	1830,1 415	#	0,40968 031	0,40968 031	81,93 606	∞
	1.0	Sample 8.d	Cal	5	11.10.2021 19:05	1	19,6 78	10365, 458	#	1,04418 687	1,04418 687	104,4 187	1049, 83
	10	Sample 9.d	Cal	6	11.10.2021 19:51	10	19,6 78	12033 5,82	#	10,0921 683	10,0921 683	100,9 217	298,6 744
	20	Sample 10.d	Cal	7	11.10.2021 20:37	20	19,6 78	20886 2,94	#	19,9539 645	19,9539 645	99,76 982	344,6 812
0,77837 1848	F 2	67 Sample 12.d	Sample	0,98 44	11.10.2021 22:08	0,984 4	19,6 32	1848,0 619	#	1,53245 849	1,53245 849		3,126 997
1,63770 8947	F 2	68 Sample 13.d	Sample	0,95 63	11.10.2021 22:54	0,956 3	19,7 24	5393,4 83	#	3,13228 213	3,13228 213		∞
		Blank3	Sample	-	11.10.2021 23:39		19,9 3	0	#				
0	P	56 Sample 15.d	Sample	1,01 76	12.10.2021 00:25	1,017 6	19,6 55	0	#				
0	P	57 Sample 16.d	Sample	1,22 2	12.10.2021 01:11	1,222	19,6 32	0	#				
0	P	58 Sample 17.d	Sample	1,27 62	12.10.2021 01:56	1,276 2	19,6 32	0	#				
		59 Sample 18.d	Sample	-	12.10.2021 02:42		19,6 78	0	#				
0	C	1 Sample 19.d	Sample	1,00 63	12.10.2021 03:27	1,006 3	19,5 64	0	#	0			
0	C	4 Sample 20.d	Sample	1,01 81	12.10.2021 04:13	1,018 1	19,4 26	0	#	0			
0	C	7 Sample 21.d	Sample	0,97 41	12.10.2021 04:59	0,974 1	19,6 55	0	#	0			
0,29956 499	C	10 Sample 22.d	Sample	1,17 8	12.10.2021 05:44	1,178	19,6 1	319,31 438	#	0,70577 512	0,70577 512		3,292 372
		19 Sample 23.d	Sample	-	12.10.2021 06:30		19,8 16	0	#				
2,71698 7267	F 4	73 Sample 24.d	Sample	1,10 09	12.10.2021 07:16	1,100 9	19,7 47	9348,8 923	#	5,98226 257	5,98226 257		8,317 871
2,18714 1849	F 4	75 Sample 25.d	Sample	0,95 01	12.10.2021 08:01	0,950 1	19,7 24	6350,0 931	#	4,15600 694	4,15600 694		7,188 14
2,46478 1228	F 4	77 Sample 26.d	Sample	1,03 27	12.10.2021 08:47	1,032 7	19,7 47	2967,8 294	#	5,09075 915	5,09075 915		10,80 168

0,96150 5811	F 2	71	Sample 27.d	Sam ple	1,14 08	12.10.2021 09:33	1,140 8	19,8 61	3502,9 348	# #	2,19377 166	2,19377 166		61,85 345
		79	Sample 28.d	Sam ple	-	12.10.2021 10:18		19,7 47	0	# #				
		Blank 4	Sample 29.d	Sam ple	-	12.10.2021 11:04		19,6 32	0	# #				
183,249 2305	G	81	Sample 30.d	Sam ple	0,92 99	12.10.2021 11:50	0,929 9	19,6 55	62260 0,98	# #	340,806 919	340,806 919		∞
36,2578 1441	G	83	Sample 31.d	Sam ple	0,90 87	12.10.2021 12:35	0,908 7	19,6 55	12765 3,3	# #	65,8949 519	65,8949 519		29,03 196
96,1843 2276	G	85	Sample 32.d	Sam ple	1,18 75	12.10.2021 13:21	1,187 5	19,6 32	42951 9,14	# #	228,437 767	228,437 767		∞
27,5309 1766	G	87	Sample 33.d	Sam ple	0,91 79	12.10.2021 14:07	0,917 9	19,6 32	92629, 029	# #	50,5412 586	50,5412 586		95,20 876
		99	Sample 34.d	Sam ple	-	12.10.2021 14:52		19,5 87	0	# #				
		13	Sample 35.d	Sam ple	1,13 33	12.10.2021 15:38		19,5 64	2143,2 938	# #	1,25616 893	1,25616 893		1,544 501
		131	Sample 36.d	Sam ple	1,11 77	12.10.2021 16:24		19,5 64	2341,1 003	# #	1,41526 229	1,41526 229		4,926 37
		132	Sample 37.d	Sam ple	1,11 83	12.10.2021 17:09		19,6 1	1746,1 388	# #	1,54348 028	1,54348 028		28,83 321
		133	Sample 38.d	Sam ple	1,05 66	12.10.2021 17:55		19,5 87	1830,1 09	# #	1,58137 703	1,58137 703		0,281 33
		134	Sample 39.d	Sam ple	1,14 68	12.10.2021 18:40		19,6 78	622,30 74	# #	1,15916 692	1,15916 692		∞
		135	Sample 40.d	Sam ple	1,18 69	12.10.2021 19:26		19,6 78	1879,8 113	# #	2,07780 455	2,07780 455		7,610 126
		136	Sample 41.d	Sam ple	1,09 6	12.10.2021 20:12		19,7 24	5407,4 244	# #	4,35242 975	4,35242 975		852,6 052
		137	Sample 42.d	Sam ple	1,01 3	12.10.2021 20:57		19,6 78	4590,0 475	# #	3,67692 571	3,67692 571		∞
		138	Sample 43.d	Sam ple	1,24 54	12.10.2021 21:43		19,8 16	4807,5 345	# #	3,62050 396	3,62050 396		∞
		139	Sample 44.d	Sam ple		12.10.2021 22:29		19,7 47	0	# #				
		140	Sample 45.d	Sam ple		12.10.2021 23:14		20,4 11	0	# #				
		Blank 5	Sample 46.d	Sam ple		13.10.2021 00:00		19,1 06	0	# #				

Table F-2: Overview over the calculated concentrations of L-PFOS in the samples in µg/kg.

	Mean	Median	Min	Max
Zooplankton	0	0	0	0
Crab	0,037	0	0	0,15
Fish st 2	1,13	0,96	0,78	1,6
Fish st 4	2,5	2,5	2,2	2,7
Gull	86	66	28	183

Table F-3: Raw data obtained from the quantification of P6MHPs in the samples. Concentrations above LOQ are highlighted as green. Concentrations above LOD are highlighted as orange, and concentrations below LOD are highlighted as red.

c (µg/kg)		Name	Data File	Type	Level	Acq. Date-Time	Exp. Conc.	RT	Resp.	M I	Calc. Conc.	Final Conc.	Accuracy	S/N
		Blank1	Sample 2.d	Sample		11.10.2021 14:31		18,601	0	#				
		Blank2	Sample 3.d	Sample		11.10.2021 15:17		18,693	0	#				
		0	Sample 4.d	Cal	1	11.10.2021 16:03	0	18,464	0	#				
		0.05	Sample 5.d	Cal	2	11.10.2021 16:48	0,05	18,693	973,61728	#	0,03844902	0,03844902	76,89804	31,33659
		0.1	Sample 6.d	Cal	3	11.10.2021 17:34	0,1	18,601	1337,8311	#	0,04734825	0,04734825	47,34825	2,050063
		0.5	Sample 7.d	Cal	4	11.10.2021 18:20	0,5	18,67	8744,3389	#	0,30650804	0,30650804	61,30161	70,06011
		1.0	Sample 8.d	Cal	5	11.10.2021 19:05	1	18,578	31598,545	#	0,88756926	0,88756926	88,75693	1880,739
		10	Sample 9.d	Cal	6	11.10.2021 19:51	10	18,647	366740,24	#	10,697263	10,697263	106,9726	1129,275
		20	Sample 10.d	Cal	7	11.10.2021 20:37	20	18,647	585106,38	#	19,6621195	19,6621195	98,3106	5809,19
0	F2	67	Sample 12.d	Sample	0,9844	11.10.2021 22:08		18,67	0	#				
0,0443325	F2	68	Sample 13.d	Sample	0,9563	11.10.2021 22:54		18,647	387,56089	#	0,0847904	0,0847904		1,276439
		Blank3	Sample 14.d	Sample	-	11.10.2021 23:39		18,693	0	#				
0	P	56	Sample 15.d	Sample	1,0176	12.10.2021 00:25		18,555	0	#				
0	P	57	Sample 16.d	Sample	1,222	12.10.2021 01:11		19,7	0	#				
0	P	58	Sample 17.d	Sample	1,2762	12.10.2021 01:56		18,624	0	#				
		59	Sample 18.d	Sample	-	12.10.2021 02:42		18,258	0	#				
0	C	1	Sample 19.d	Sample	1,0063	12.10.2021 03:27		18,647	0	#				
0	C	4	Sample 20.d	Sample	1,0181	12.10.2021 04:13		18,578	0	#				
0	C	7	Sample 21.d	Sample	0,9741	12.10.2021 04:59		18,281	0	#				
0	C	10	Sample 22.d	Sample	1,178	12.10.2021 05:44		19,539	0	#				
		19	Sample 23.d	Sample	-	12.10.2021 06:30		18,098	0	#				
0,139402	F4	73	Sample 24.d	Sample	1,1009	12.10.2021 07:16		18,509	1354,4843	#	0,30693539	0,30693539		11,9015
0,087809	F4	75	Sample 25.d	Sample	0,9501	12.10.2021 08:01		18,349	710,79199	#	0,16685458	0,16685458		2,549494
0,0690114	F4	77	Sample 26.d	Sample	1,0327	12.10.2021 08:47		18,464	226,45658	#	0,1425361	0,1425361		0,397624

0,0419 738	F 2	71	Sample 27.d	Sam ple	1,14 08	12.10.2021 09:33	18,6 01	427,55 574	# #	0,09576 752	0,09576 752	1,219 496
		79	Sample 28.d	Sam ple	-	12.10.2021 10:18	18,7 38	0	# #			
		Blank4	Sample 29.d	Sam ple	-	12.10.2021 11:04	18,4 18	0	# #			
9,7875 694	G	81	Sample 30.d	Sam ple	0,92 99	12.10.2021 11:50	18,6 01	93483, 759	# #	18,2029 215	18,2029 215	60,11 088
0,9551 89	G	83	Sample 31.d	Sam ple	0,90 87	12.10.2021 12:35	18,5 78	9428,2 144	# #	1,73596 04	1,73596 04	∞
3,8341 085	G	85	Sample 32.d	Sam ple	1,18 75	12.10.2021 13:21	18,6 24	48120, 251	# #	9,10600 777	9,10600 777	∞
0,6918 296	G	87	Sample 33.d	Sam ple	0,91 79	12.10.2021 14:07	18,6 24	6518,0 236	# #	1,27006 078	1,27006 078	∞
		99	Sample 34.d	Sam ple	-	12.10.2021 14:52	18,8 07	0	# #			
		13	Sample 35.d	Sam ple	1,13 33	12.10.2021 15:38	18,6 47	6433,9 22	# #	1,10055 966	1,10055 966	2264, 596
		131	Sample 36.d	Sam ple	1,11 77	12.10.2021 16:24	18,6 01	9785,9 862	# #	1,76488 114	1,76488 114	734,1 371
		132	Sample 37.d	Sam ple	1,11 83	12.10.2021 17:09	18,5 78	5810,3 77	# #	1,55891 028	1,55891 028	534,5 391
		133	Sample 38.d	Sam ple	1,05 66	12.10.2021 17:55	18,5 55	4596,1 375	# #	1,21304 689	1,21304 689	∞
		134	Sample 39.d	Sam ple	1,14 68	12.10.2021 18:40	18,6 7	2134,8 623	# #	1,13780 24	1,13780 24	812,2 452
		135	Sample 40.d	Sam ple	1,18 69	12.10.2021 19:26	18,6 24	4750,1 06	# #	1,66673 711	1,66673 711	18,12 456
		136	Sample 41.d	Sam ple	1,09 6	12.10.2021 20:12	18,6 7	6255,3 254	# #	1,70494 214	1,70494 214	18,26 507
		137	Sample 42.d	Sam ple	1,01 3	12.10.2021 20:57	18,6 24	5110,3 764	# #	1,37376 215	1,37376 215	7,721 964
		138	Sample 43.d	Sam ple	1,24 54	12.10.2021 21:43	18,6 24	3360,3 964	# #	0,85243 799	0,85243 799	65,99 411
		139	Sample 44.d	Sam ple		12.10.2021 22:29	18,3 26	0	# #			
		140	Sample 45.d	Sam ple		12.10.2021 23:14	18,1 89	0	# #			
		Blank5	Sample 46.d	Sam ple		13.10.2021 00:00	18,2 35	0	# #			

Table F-4: Overview over the calculated concentrations of P6MHPs in the samples in µg/kg.

	Mean	Median	Min	Max
Zooplankton	0	0	0	0
Crab	0	0	0	0
Fish st 2	0,029	0,042	0,000	0,044
Fish st 4	0,099	0,088	0,069	0,14
Gull	3,8	2,4	0,69	9,8

Table F-5: Raw data obtained from the quantification of P-1/3/5-HpS in the samples. Concentrations above LOQ are highlighted as green. Concentrations above LOD are highlighted as orange, and concentrations below LOD are highlighted as red.

Sample					P1/P3/P5-MHpS Method					P1/P3/P5-MHpS Results				
c (µg/kg)		Na me	Data File	Type	Level/w eight	Acq. Date- Time	Exp. Conc.	RT	Resp.	MI	Calc. Conc.	Final Conc.	Accur acy	S/N
		Blan k1	Sample 2.d	Sam ple		11.10.2021 14:31		18,1 64	0	SAN N				
		Blan k2	Sample 3.d	Sam ple		11.10.2021 15:17		18,4 16	0	SAN N				
		0	Sample 4.d	Cal	1	11.10.2021 16:03	0	18,6 9	0	SAN N				
		0.05	Sample 5.d	Cal	2	11.10.2021 16:48	0,15	18,1 64	11615, 02	USA NN	0,2539 8949	0,2539 8949	169,3 263	4,216 851
		0.1	Sample 6.d	Cal	3	11.10.2021 17:34	0,3	18,1 64	19919, 008	USA NN	0,3011 4059	0,3011 4059	100,3 802	6,598 93
		0.5	Sample 7.d	Cal	4	11.10.2021 18:20	1,5	18,1 87	10663 7,25	USA NN	0,9742 1904	0,9742 1904	64,94 794	109,5 405
		1.0	Sample 8.d	Cal	5	11.10.2021 19:05	3	18,1 87	38914 4,66	SAN N	2,5551 1278	2,5551 1278	85,17 043	414,3 568
		10	Sample 9.d	Cal	6	11.10.2021 19:51	30	18,2 1	48577 41,4	USA NN	31,298 169	31,298 169	104,3 272	8519, 852
		20	Sample 10.d	Cal	7	11.10.2021 20:37	60	18,2 1	80188 99,5	USA NN	59,386 0387	59,386 0387	98,97 673	943,7 838
0,209 8	F 2	67	Sample 12.d	Sam ple	0,98	11.10.2021 22:08		18,2 1	4224,1 44	SAN N	0,4131 3511	0,4131 3511		2,254 855
0,271	F 2	68	Sample 13.d	Sam ple	0,96	11.10.2021 22:54		18,1 87	8023,8 989	SAN N	0,5183 3739	0,5183 3739		4,107 28
#### ##		Blan k3	Sample 14.d	Sam ple	-	11.10.2021 23:39		18,1 41	0	SAN N				
0	P	56	Sample 15.d	Sam ple	1,02	12.10.2021 00:25		18,1 64	0	SAN N				
0	P	57	Sample 16.d	Sam ple	1,22	12.10.2021 01:11		19,6 75	0	SAN N				
0	P	58	Sample 17.d	Sam ple	1,28	12.10.2021 01:56		19,6 06	0	SAN N				
#### ##		59	Sample 18.d	Sam ple	-	12.10.2021 02:42		18,1 87	0	SAN N				
0	C	1	Sample 19.d	Sam ple	1,01	12.10.2021 03:27		18,2 1	0	SAN N				
0	C	4	Sample 20.d	Sam ple	1,02	12.10.2021 04:13		18,4 16	0	SAN N				
0	C	7	Sample 21.d	Sam ple	0,97	12.10.2021 04:59		17,0 88	0	SAN N				
0	C	10	Sample 22.d	Sam ple	1,18	12.10.2021 05:44		19,6 75	0	SAN N				
#### ##		19	Sample 23.d	Sam ple	-	12.10.2021 06:30		18,2 33	0	SAN N				

0,4428	F4	73	Sample 24.d	Sample	1,1	12.10.2021 07:16	18,164	16509,364	SAN N	0,97495234	0,97495234	2,660423
0,2556	F4	75	Sample 25.d	Sample	0,95	12.10.2021 08:01	18,279	6303,659	SAN N	0,48567723	0,48567723	4,742829
0,3958	F4	77	Sample 26.d	Sample	1,03	12.10.2021 08:47	18,21	4972,8538	SAN N	0,81753516	0,81753516	0,988684
0,2432	F2	71	Sample 27.d	Sample	1,14	12.10.2021 09:33	18,21	8546,3398	SAN N	0,55493755	0,55493755	1,770549
####		79	Sample 28.d	Sample	-	12.10.2021 10:18	18,164	0	SAN N			
####		Blank4	Sample 29.d	Sample	-	12.10.2021 11:04	18,233	0	SAN N			
26,792	G	81	Sample 30.d	Sample	0,93	12.10.2021 11:50	18,164	1160533,7	USA NN	49,8279441	49,8279441	318,2729
2,2135	G	83	Sample 31.d	Sample	0,91	12.10.2021 12:35	18,187	95498,059	USA NN	4,02275457	4,02275457	9,482419
6,8636	G	85	Sample 32.d	Sample	1,19	12.10.2021 13:21	18,187	387957,6	USA NN	16,3009598	16,3009598	27,05782
1,9672	G	87	Sample 33.d	Sample	0,92	12.10.2021 14:07	18,141	80759,503	USA NN	3,61134831	3,61134831	9,681877
####		99	Sample 34.d	Sample	-	12.10.2021 14:52	18,233	0	SAN N			
1,8607		13	Sample 35.d	Sample	1,13	12.10.2021 15:38	18,118	108395,76	SAN N	4,21753632	4,21753632	7,419688
2,1097		131	Sample 36.d	Sample	1,12	12.10.2021 16:24	18,164	115078,74	SAN N	4,71591611	4,71591611	13,56413
2,4434		132	Sample 37.d	Sample	1,12	12.10.2021 17:09	18,164	90206,362	SAN N	5,46498091	5,46498091	125,6547
2,5063		133	Sample 38.d	Sample	1,06	12.10.2021 17:55	18,187	88947,527	SAN N	5,29624598	5,29624598	10,50027
2,3449		134	Sample 39.d	Sample	1,15	12.10.2021 18:40	18,21	44779,584	SAN N	5,37818217	5,37818217	4,840539
2,182		135	Sample 40.d	Sample	1,19	12.10.2021 19:26	18,233	65221,423	SAN N	5,17970844	5,17970844	11,13425
2,4678		136	Sample 41.d	Sample	1,1	12.10.2021 20:12	18,233	87809,74	SAN N	5,40939061	5,40939061	8,347802
2,4252		137	Sample 42.d	Sample	1,01	12.10.2021 20:57	18,301	80710,765	SAN N	4,91353895	4,91353895	5,528126
1,9517		138	Sample 43.d	Sample	1,25	12.10.2021 21:43	18,279	84993,099	SAN N	4,86117309	4,86117309	6,822383
		139	Sample 44.d	Sample		12.10.2021 22:29	18,347	0	SAN N			
		140	Sample 45.d	Sample		12.10.2021 23:14	18,324	0	SAN N			
		Blank5	Sample 46.d	Sample		13.10.2021 00:00	18,233	0	SAN N			

Table F-6: Overview over the calculated concentrations of P-1/3/5-HpS in the samples in µg/kg.

	Mean	Median	Min	Max
Plankton	0	0	0	0
Crab	0	0	0	0
Fish st 2	0,24	0,24	0,21	0,27
Fish st 4	0,36	0,40	0,26	0,44
Gull	9,5	4,5	2,0	27

Table F-7: Raw data obtained from the quantification of P-44/45/55-DMHxS in the samples. Concentrations above LOQ are highlighted as green. Concentrations above LOD are highlighted as orange, and concentrations below LOD are highlighted as red.

Sample				P44/P45/P55-DMHxS Method					P44/P45/P55-DMHxS Results				
C (µg/kg)	Name	Data File	Type	Level	Acq. Date-Time	Exp. Conc.	RT	Resp.	MI	Calc. Conc.	Final Conc.	Accuracy	S/N
	Blank1	Sample 2.d	Sample		11.10.2021 14:31		17,2 49	0	#				
	Blank2	Sample 3.d	Sample		11.10.2021 15:17		16,9 28	0	#				
	0	Sample 4.d	Cal	1	11.10.2021 16:03	0	17,2 72	0	#				
	0.05	Sample 5.d	Cal	2	11.10.2021 16:48	0,15	17,2 26	31326,929	#	0,28108 909	0,28108 909	187,3 927	4,339 885
	0.1	Sample 6.d	Cal	3	11.10.2021 17:34	0,3	17,4 32	53384,918	#	0,33601 882	0,33601 882	112,0 063	11,20 306
	0.5	Sample 7.d	Cal	4	11.10.2021 18:20	1,5	17,4 32	235051,51	#	0,96224 705	0,96224 705	64,14 98	148,8 202
	1.0	Sample 8.d	Cal	5	11.10.2021 19:05	3	17,4 55	910216,77	#	2,63235 262	2,63235 262	87,74 509	650,4 459
	10	Sample 9.d	Cal	6	11.10.2021 19:51	30	17,4 55	109638 42	#	31,0238 181	31,0238 181	103,4 127	11771,58
	20	Sample 10.d	Cal	7	11.10.2021 20:37	60	17,4 78	183045 62	#	59,5194 093	59,5194 093	99,19 902	113,9 051
0	F2	67	Sample 12.d	Sample	0,98 44		11.10.2021 22:08		18,2 1	0	#		
0	F2	68	Sample 13.d	Sample	0,95 63		11.10.2021 22:54		18,1 87	0	#		
####		Blank3	Sample 14.d	Sample	-		11.10.2021 23:39		17,2 72	0	#		
0	P	56	Sample 15.d	Sample	1,01 76		12.10.2021 00:25		13,3 12	0	#		
0	P	57	Sample 16.d	Sample	1,22 2		12.10.2021 01:11		15,9 21	0	#		
0	P	58	Sample 17.d	Sample	1,27 62		12.10.2021 01:56		15,8 98	0	#		

#### #		59	Sample 18.d	Sam ple	-	12.10.2021 02:42		18,1 87	0	# #				
0	C	1	Sample 19.d	Sam ple	1,00 63	12.10.2021 03:27		16,9 97	0	# #				
0	C	4	Sample 20.d	Sam ple	1,01 81	12.10.2021 04:13		17,0 66	0	# #				
0	C	7	Sample 21.d	Sam ple	0,97 41	12.10.2021 04:59		17,0 88	0	# #				
0	C	10	Sample 22.d	Sam ple	1,17 8	12.10.2021 05:44		19,6 75	0	# #				
#### #		19	Sample 23.d	Sam ple	-	12.10.2021 06:30		17,2 94	0	# #				
0,244	F 4	73	Sample 24.d	Sam ple	1,10 09	12.10.2021 07:16		16,9 28	16247, 601	# #	0,53791 544	0,53791 544		0,826 345
0	F 4	75	Sample 25.d	Sam ple	0,95 01	12.10.2021 08:01		18,2 79	0	# #				
0	F 4	77	Sample 26.d	Sam ple	1,03 27	12.10.2021 08:47		18,2 1	0	# #				
0	F 2	71	Sample 27.d	Sam ple	1,14 08	12.10.2021 09:33		18,2 1	0	# #				
#### #		79	Sample 28.d	Sam ple	-	12.10.2021 10:18		17,3 4	0	# #				
#### #		Blan k4	Sample 29.d	Sam ple	-	12.10.2021 11:04		17,2 03	0	# #				
0,585	G	81	Sample 30.d	Sam ple	0,92 99	12.10.2021 11:50		17,3 4	47564, 387	# #	1,08825 922	1,08825 922		∞
0,15	G	83	Sample 31.d	Sam ple	0,90 87	12.10.2021 12:35		17,3 4	4371,5 963	# #	0,27225 659	0,27225 659		0,021 459
0,175	G	85	Sample 32.d	Sam ple	1,18 75	12.10.2021 13:21		17,2 72	12060, 615	# #	0,41503 953	0,41503 953		0,065 408
0,128	G	87	Sample 33.d	Sam ple	0,91 79	12.10.2021 14:07		17,4 55	2096,9 669	# #	0,23416 048	0,23416 048		0,075 966
		99	Sample 34.d	Sam ple	-	12.10.2021 14:52		17,2 26	0	# #				
		13	Sample 35.d	Sam ple	1,13 33	12.10.2021 15:38		17,4 09	272836 ,72	# #	4,65466 53	4,65466 53		70,42 545
		131	Sample 36.d	Sam ple	1,11 77	12.10.2021 16:24		17,4 09	258323 ,25	# #	4,66332 21	4,66332 21		22,75 434
		132	Sample 37.d	Sam ple	1,11 83	12.10.2021 17:09		17,4 32	205931 ,89	# #	5,48990 252	5,48990 252		6,593 881
		133	Sample 38.d	Sam ple	1,05 66	12.10.2021 17:55		17,4 32	226013 ,1	# #	5,90025 785	5,90025 785		18,00 221
		134	Sample 39.d	Sam ple	1,14 68	12.10.2021 18:40		17,4 32	98395, 978	# #	5,20774 232	5,20774 232		8,096 239
		135	Sample 40.d	Sam ple	1,18 69	12.10.2021 19:26		17,4 55	165058 ,44	# #	5,74782 21	5,74782 21		18,33 805
		136	Sample 41.d	Sam ple	1,09 6	12.10.2021 20:12		17,4 78	200930 ,46	# #	5,44647 331	5,44647 331		8,040 569
		137	Sample 42.d	Sam ple	1,01 3	12.10.2021 20:57		17,5	195004 ,07	# #	5,21396 104	5,21396 104		6,369 834

	138	Sample 43.d	Sample	1,24 54	12.10.2021 21:43		17,5	184155 ,01	# #	4,64612 3	4,64612 3		5,936 276
	139	Sample 44.d	Sample		12.10.2021 22:29		17,3 86	0	# #				
	140	Sample 45.d	Sample		12.10.2021 23:14		16,8 14	0	# #				
	Blank5	Sample 46.d	Sample		13.10.2021 00:00		17,3 4	0	# #				

Table F-8: Overview over the calculated concentrations of P-44/45/55-DMHxS in the samples in $\mu\text{g}/\text{kg}$.

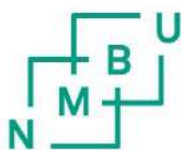
	Mean	Median	Min	Max
Planton	0	0	0	0
Crab	0	0	0	0
Fish st 2	0	0	0	0
Fish st 4	0,081	0	0	0,24
Gull	0,26	0,16	0,13	0,59

Appendix G – Sample protocol

Table G-1: Overview over the samples run, the sample type, weight and addition of ISTDs and STDs

Sample run number	Sample preparation number	Sample code	Sample type	Weight (g)	ISTD added	STDs spiked
1	-	Mix 10	STDs mix	-	N	N
2	-	-	Instrument blank	-	N	N
3	-	-	Instrument blank	-	N	N
4	c0	Cal 0	Calibration	-	Y	N
5	c0.05	Cal 0.05	Calibration	-	Y	N
6	c0.1	Cal 0.1	Calibration	-	Y	N
7	c0.5	Cal 0.5	Calibration	-	Y	N
8	c1.0	Cal 1.0	Calibration	-	Y	N
9	c10	Cal 10	Calibration	-	Y	N
10	c20	Cal 20	Calibration	-	Y	N
11	-	Mix 10	STDs mix	-	N	N
12	67	F-2-1	Fish	0,9844	Y	N
13	68	F-2-2	Fish	0,9563	Y	N
14	-	-	Instrument blank	-	N	N
15	56	P-4-1	Zooplankton	1,0176	Y	N
16	57	P-4-2	Zooplankton	1,222	Y	N
17	58	P-4-3	Zooplankton	1,2762	Y	N
18	59	S-B	Procedural blank	-	Y	N
19	1	C-St4-1-1-W	Crab	1,0063	Y	N
20	4	C-St4-2-1-W	Crab	1,0181	Y	N
21	7	C-St4-4-1-W	Crab	0,9741	Y	N
22	10	C-St4-5-1-W	Crab	1,178	Y	N
23	19	C-B-W-1	Procedural blank	-	Y	N
24	73	F-3-4-1	Fish	1,1009	Y	N
25	75	F-3-5	Fish	0,9501	Y	N
26	77	F-3-7	Fish	1,0327	Y	N
27	71	F-2-3	Fish	1,1408	Y	N

28	79	F-B-1	Procedural blank	-	Y	N
29	-	-	Instrument blank	-	N	N
30	81	G-1-1	Gull	0,9299	Y	N
31	83	G-2-1	Gull	0,9087	Y	N
32	85	G-3-1	Gull	1,1875	Y	N
33	87	G-4-1	Gull	0,9179	Y	N
34	99	-	Instrument blank	-	N	N
35	130	P-St4- R-40	Recovery	1,1333	Y	Y
36	131	P-St4- R-40	Recovery	1,1177	Y	Y
37	132	P-St4- R-40	Recovery	1,1183	Y	Y
38	133	C-St4- 1-R-40	Recovery	1,0566	Y	Y
39	134	C-St4- 1-R-40	Recovery	1,1468	Y	Y
40	135	C-St4- 1-R-40	Recovery	1,1869	Y	Y
41	136	F-St2-3- R-40	Recovery	1,096	Y	Y
42	137	F-St2-3- R-40	Recovery	1,013	Y	Y
43	138	F-St2-3- R-40	Recovery	1,2454	Y	Y
44	139	R-B-3	Procedural blank	-	Y	N
45	140	R-B-4	Procedural blank	-	Y	N
46	-	Blank	Instrument blank	-	N	N



Norwegian University
of Life Sciences

Master's Thesis 2021 60 ECTS

Faculty of Chemistry, Biotechnology and Food Science

Distribution of perfluorooctanesulfonate (PFOS) isomers in a Norwegian arctic food web

Fedor Lennikov

Chemistry